Reservoir Characterization of Sawan Gas Field using Seismic Inversion and Machine Learning Algorithms, Central Indus Basin, Pakistan

ABDUL BASIT

01-262212-011

Department of Earth and Environmental Sciences

Bahria University, Islamabad

2024

Reservoir Characterization of Sawan Gas Field using Seismic Inversion and Machine Learning Algorithms, Central Indus Basin, Pakistan

ABDUL BASIT

01-262212-011

A thesis submitted to Bahria University, Islamabad in partial fulfillment of the requirement for the degree of Master of Science in Geophysics

Department of Earth and Environmental Sciences

Bahria University, Islamabad

2024

APPROVAL FOR EXAMINATION

Scholar's Name: ABDUL BASIT

Registration No. 49655

Programme of Study: MS GEOPHYSICS

Thesis Title: Reservoir Characterization of Sawan Gas Field using Seismic Inversion and Machine Learning Algorithms, Central Indus Basin, Pakistan

It is to certify that the above scholar's thesis has been completed to my satisfaction and, to my belief, its standard is appropriate for submission for examination. I have also conducted a plagiarism test of this thesis using HEC prescribed software and found similarity index 15% that is within the permissible limit set by the HEC for the MS degree thesis. I have also found the thesis in a format recognized by the BU for the MS thesis.

Principal Supervisor's Signature: _____

Date: _____

Name: _____

AUTHOR'S DECLARATION

I, **"Abdul Basit"** hereby state that my MS thesis titled **"Reservoir Characterization of Sawan Gas Field using Seismic Inversion and Machine Learning Algorithms, Central Indus Basin, Pakistan"** is my own work and has not been submitted previously by me for taking any degree from this university **Bahria University Islamabad** or anywhere else in the country/world. At any time if my statement is found to be incorrect even after my graduation, the University has the right to withdraw/cancel my MS degree.

Name of scholar: Abdul Basit

Date:_____

PLAGIARISM UNDERTAKING

I solemnly declare that research work presented in the thesis titled **"Reservoir Characterization of Sawan Gas Field using Seismic Inversion and Machine Learning Algorithms, Central Indus Basin, Pakistan"** is solely my research work with no significant contribution from any other person. Small contribution / help wherever taken has been duly acknowledged and that complete thesis has been written by me.

I understand the zero-tolerance policy of the HEC and Bahria University towards plagiarism. Therefore, I as an Author of the above titled thesis declare that no portion of my thesis has been plagiarized and any material used as reference is properly referred to / cited.

I undertake that if I am found guilty of any formal plagiarism in the above titled thesis even after award of MS degree, the university reserves the right to withdraw / revoke my MS degree and that HEC and the University has the right to publish my name on the HEC / University website on which names of scholars are placed who submitted plagiarized thesis.

Scholar / Author's Sign: _____

Name of the Scholar: Abdul Basit

DEDICATION

With all my love and admiration this work is unequivocally dedicated to my family.

ACKNOWLEDGEMENTS

All glorification and reverence belong to Allah S.W.T and it is of utmost significance to bow my head before Allah Almighty, who is the solitary provider of all erudition. The Greatest of all, who refined my heart with enhanced perceptions and blessed me robustness to complete my research. Countless salutations are upon the Holy Prophet Muhammad (S.A.W.W), the foundation of knowledge who always guided His Ummah to seek knowledge.

I am considerably obliged and thankful to my honorable supervisor Dr Muhammad Fahad Mehmood and my Co-supervisor Mr. Muyassar Hussain for their relentless assistance, expert guidance, continuous encouragement, devotion, and supervision during the immensely crucial stage of my degree. I substantially admire the level of power gap that you retained throughout the study and made me quite comfortable to contact you any time for any complications encountered during my research work. I will eternally commemorate the amiable attitude and endorsement during the entire period.

Further to this, I am significantly grateful to Prof. Syed Umair Ullah Jamil, Head of Department of Earth and Environmental Sciences, Bahria University, Islamabad for his peculiar succor. My heartfelt gratitude goes to my teachers and fellow geologists for the virtuous and influential encouragement, assistance and collaboration during research work.

ABSTRACT

The study's primary goal is to identify the thin sands packages of B and C Intervals of Lower Goru Formation of Sawan Gas Field, by using machine learning along with reservoir characterization by performing seismic interpretation, seismic inversion, petrophysics, Rock physics modelling and using machine learning algorithms. The Sawan Gas Field is situated within the Central Indus Basin of Pakistan, and its geological setting is characterized by extensional tectonic processes. Following the completion of seismic interpretation, seismic inversion, and petrophysical analysis, the findings indicate that the C Interval of the Lower Goru Formation within the Sawan Gas Field exhibits a more substantial hydrocarbon potential when contrasted with the B-Interval. Rock physics modeling have used for the prediction of P and S waves variations and how Poisson's ratio occurs. Rock physics depicted the missing log prediction like S-wave specifically and fluid substitution also occurred with different conditions to confirm reservoir availability. Model Based Inversion (MBI) has been used to predict and confirm more better results came from seismic interpretation. The wavelet was extracted from the control line and the correlation occurred. LFM (Low Frequency Models) have been generated as well. Afterwards Quality control of data occurred by inverted techniques. Lastly to confirm results with seismic inversion technique, Machine learning (PNN) based on Bayesian classifier method which gives reliable prediction of petrophysical properties, so it is used predict Volume of clay prediction, Porosity prediction and Saturation of water was predicted by Actual and Predicted values

TABLE OF CONTENTS

APPROVAL FOR EXAMINATION i

AUTHOR'S DECLARATION ii

PLAGIARISM UNDERTAKING iii

DEDICATION iv

ACKNOWLEDGEMENTS v

ABSTRACT vi

TABLE OF CONTENTS vii

LIST OF TABLES xii

LIST OF FIGURES xiii

CHAPTER 01 1

INTRODUCTION 1

1.1. Overview 1

1.2. Location Map 3

1.3. Exploration History 4

1.4. Data Set: 5

1.4.1. Seismic Data: 5

1.4.2. Well Data: 5

1.5 Software Used 6

1.6 Literature review 6

1.7 Purpose of research 7

1.8. Base Map: 7

1.9. Objectives of the Study: 8

1.10. Methodology 9

CHAPTER 02 11

GEOLOGY OF STUDY AREA 11

2.1. Introduction 11

2.2. Geological Settings 11

2.3. Tectonic Settings 13

2.4. Stratigraphy of Lower Indus Basin 16

2.5. Petroleum Play 17

2.5.1 Source Rock: 18

2.5.2 Reservoir Rock: 18

2.5.3 Trap and Seal: 18

CHAPTER 3 20

SEISMIC DATA INTERPRETATION 20

3.1 Seismic Interpretation's Workflow 21

3.1.1 Loading of Seismic Data 22

3.1.2 Base Map 22

3.1.3 Synthetic Seismogram 23

3.1.4 Horizon and fault marking 25

Interpreted sections: 25

3.1.5 Preparation of Contour Maps 27

3.1.6 Interpretation of C-interval maps 28

3.1.7 Interpretation of B-interval maps 31

CHAPTER 04 35

PETROPHYSICS 35

4.1 Introduction 35

4.2 Petrophysical Analysis 36

4.3 Lithology identification 36
4.4 Porosity 37
4.4.1 Density Porosity 38
4.4.2 Sonic Porosity 39
4.4.3 Effective Porosity 40
4.4.4 Neutron Porosity 40
4.4.5 Total Porosity 40
4.4.6 Saturation of Water 41
4.4.7 Pickett Cross Plot Method: 42
4.4.8 Calculation of Archie Water Saturation (Sw) 43
4.4.9 Calculation of Hydrocarbon Saturation (Sh) 44
4.5 Petrophysical Interpretation of B interval 44
4.5.1 Petrophysical Interpretation of B Interval Sawan 01 45
4.6 Petrophysical interpretation of C interval 46
4.6.1 Petrophysical Interpretation of C Interval Sawan 01 47
4.6.2 Petrophysical Interpretation of C Interval Sawan 07 48
4.7 Results of Petrophysical Interpretation 49
CHAPTER NO 5 50
ROCK PHYSICS AND FLUID REPLACEMENT MODELING 50
5.1 Introduction 50
5.2 Fluid replacement modeling 50
5.3 Workflow of Rock Physics 51
5.4 Scenarios in for fluid substitution 51
5.4.1 Insitu case (80% gas 20% water) 51
5.4.2 Gas 100 % and water 0 % 52

5.4.3 50% gas 50% water case 53
5.4.4 Outcome 54
CHAPTER NO 6 55
SEISMIC INVERSION TECHNIQUE FOR RESERVOIR CHARACTERIZATION 55
6.1 Introduction 55
6.1.1 Seismic inversion's purpose 57
6.2 Post Stack Inversion 57
6.3 Model Based Inversion 58
6.4 Methodology adopted for Model Based Inversion 59
6.4.1 Seismic and Well Data Loading 59
6.4.2 Loading of Horizons 60
6.4.3 Extraction of statistical wavelet 60
6.4.4 Seismic to Well Correlation 60
6.4.5 Initial Low Frequency Model 61
6.4.6 Inversion Analysis 64
6.4.7 Results of Model Based Inversion 66
6.4.8 Slice of C interval 68
CHAPTER NO 7 70
MACHINE LEARNING IMPLEMENTATION FOR RESERVOIR CHARACTERIZATION 70
7.1 Introduction 70
7.2 Methodology 70
7.2.1 Probabilistic Neural Network (PNN) 70
7.2.2 Volume of Clay prediction using PNN (Machine learning) 71
7.3 Results 73

7.3.1 Porosity prediction using PNN (Machine learning) 74

7.3.2 Sw prediction using PNN (Machine learning) 77

CONCLUSIONS 81

REFERENCES 82

LIST OF TABLES

TABLE NO.	TITLE	PAGE
1.1	Well data used in reservoir characterization.	05
2.1	Generalized stratigraphy of the Lower Indus Basin (Kadri, 1995).	16
4.1	Different transient time at different matrix is as follow	38
4.2	Result of petrophysical analysis of reservoir zones	48

LIST OF FIGURES

Figure 1.1: Map showing location of Sawan field (after Berger et al., 2009). 3
Figure 3.1 Workflow adopted for seismic interpretation adopted during research. 21
Figure 3.2 Base map of the study area showing the distribution of in lines and crossline along with type of well. 23
Figure 3.3 Synthetic Seismogram of Sawan-07 25
Figure 3.4 Seismic section along with horizons of interest and faults at inline-724. 26
Figure 3.5 Seismic section of Xline-932 with well location of Sawan- 01, Sawan-07 and Sawan-08 along with the Upper Goru formation and C and B Intervals. 27
Figure 3.7 Depth contour map of C-Sands. 30
Figure 3.9 Depth contour map of B-Sand that is member of Lower Goru formation. 33
Figure 4.3 Petrophysical analysis of Sawan 01 on B-Interval of Lower Goru Formation. ..45
Figure 4.5 Petrophysical analysis of Sawan-7 C-Interval of Lower Goru Formation. 48
Figure 5.1 Fluid replacement workflow 51
Figure 5.2 Depicts that Insitu condition holds substitution of 80% Gas and 20% water scenario. 52
Figure 5.3 Depicts that substitution of 100% Gas and 0% water scenario. 53
Figure 5.4 Depicts that substitution of 50% Gas and 50% water scenario. 54
Figure 6.1 Generalized workflow of seismic inversion (Veeken and Silva, 2004). 56
Figure 6.2 Workflow Adopted for Modal Based Inversion. 59
Figure 6.3 Correlation of seismic data with Sawan-07 well. 61
Figure 6.4 Low Frequency model with well location of Sawan-07 63
Figure 6.5 Model based inversion analysis of Sawan-07 65
Figure 6.6 Final Computed impedance model at Sawan-07 Well location. 67
Figure 6.7 3D cube slice for C Interval showing variation for P-Impedance. 68

Figure 7.1 Cross plot of Actual Volume of Clay and Predicted Volumetric analysis of Clay (modeled). 72
Figure 7.2 Training result of PNN of Actual Volume of Clay and Predicted Volumetric analysis of Clay(modeled). 73
Figure 7.3 depicts that values ranging from 0.62 % to 0.68% which is holds very good results of C sand in Sawan-07. 74
Figure 7.4 Training result of PNN modeled porosity(red) and actual porosity (black)..... 75
Figure 7.5 Cross plot of actual porosity and predicted porosity (modeled). 76
Figure 7.6 depicits that values ranging from 0.203 % to 0.215% porosity which is holding very good results of in C interval in Sawan-07..... 77
Figure 7.7 Training result of PNN modeled Saturation of Water, actual Saturation of Water. 78
Figure 7.8 Cross plot of Actual Water Saturation with Predicted Water Saturation (modeled). 79
Figure 7.9 depicits that values ranging from 0.31% to 0.42% of predicted water Saturation which is holding very goodresults of C sand interval in Sawan-07. 80

CHAPTER 01

INTRODUCTION

1.1. Overview

Geophysical methods play a vital role in exploring subsurface reserves such as hydrocarbons and minerals. Techniques to explore hydrocarbons involve the examination of distant areas of the Earth through physical measurements, typically conducted on the surface. Additionally, they encompass the interpretation of these measurements to understand subsurface structures and phenomena. The Geophysical technique closely resembles remote sensing, as it involves collecting subsurface information through measurements taken from the surface. Geoscientists employ various methods for exploration, including magnetic, gravity, resistivity, among others. Among these, the seismic reflection method stands out as a widely utilized and efficient tool, contributing significantly to addressing the economic challenges faced by the country. Earth investigation by geophysical method requires taking measurements to inspect the variation both horizontally and vertically through calculating its physical properties (Bust et al., 2010).

The interpretation of 3D seismic data has evolved into a crucial tool for hydrocarbon exploration in the petroleum industry. Undoubtedly, hydrocarbon exploration serves as a cornerstone for the economy, particularly in developing countries like Pakistan. Our objective is to furnish petroleum engineers with a 3D geological model for effective well planning and reservoir performance simulation. The seismic method, initially explored by exploration geophysicists in 1915, has proven invaluable for imaging concealed subsurface geological features and identifying structural and stratigraphic traps (Coffeen, 1986). Seismic surveys, primarily conducted for hydrocarbon exploration, present data as a time series of

reflections through the subsurface (Leowenthal et al., 1987; Keskes et al., 1982). Three-dimensional (3D) seismic surveys offer numerous advantages and are applied throughout the exploration to development phases, aiding in detailed reservoir characterization. The underlying concept involves representing the subsurface structure as a simplified model consisting of resolvable parameters (Dorn, 1998).

Seismic interpretation is carried out to comprehensively determine and map the reservoir's location, trapping mechanism, and conduct seal analysis in the study area. The reservoir mapping is presented as both time and depth structure maps. Formation interfaces and faults are integral components of subsurface mapping (Stewart, 2012). Typically, seismic interpretation is a rapid process in less complex geological areas but may require a more deliberate and careful approach in geologically intricate zones, such as those with low impedance. Reservoir characterization is key to determining the Gross pay zone volume within the reservoir, which has the potential to effectively store hydrocarbons. Throughout the interpretation, petrophysical parameters like fluid saturation, porosity, permeability, and volume of shale/clay are correlated with seismic data at the well location, often using synthetic seismograms. These correlations are then extended to the entire section (Eshimokhai, 2012; Schlumberger, 1989). The interconnected network of pores plays a crucial role in fluid storage and transmission (Donaldson and Tiab, 2004). Integrating fluid properties with detailed information on permeability and porosity forms the foundation for productive field development and accurate future field predictions (Benedicuts, 2007). While conducting a core analysis for the entire reservoir may not be feasible, the interpretation of well data proves valuable in leveraging essential information and minimizing the risks associated with uncertainty. Seismic inversion has emerged as a crucial tool for reservoir characterization, experiencing increased utilization in oil and gas exploration over the past decade. The main goal of seismic inversion is to transform all of the seismic data into different quantitative characteristics of the rock. Inversion is a technique employed for predicting, calculating, and drawing inferences about physical parameters based on real data (Sen, 2006). Through inversion, we achieve a more accurate estimation of reservoir properties such as porosity, volumetrics, water saturation, etc. Additionally, inversion allows for the assessment of uncertainties and risks (Pendrel, 2000). Various inversion algorithms

play a significant role in providing a valuable link in reservoir management and development (Pendrel, 2000).

1.2. Location Map

The research area is situated within the Thar Desert, Khairpur district, Sindh, with geographical coordinates ranging from 27°17'14.424" N to 26°55'34.3452" N and 69°18' 44.0676" E to 69°18' 40.464" E. As Rahman and Ibrahim noted in 2009, two major strike-slip faults divide the Sawan field into three parts: south, center, and north. Geologically, this area is located on the southeastern flank of the Jacobabad-Khairpur High, which runs north to south. In the Middle Indus Basin, the Sawan delta complex is a platform slope.

Sawan Gas field was uncovered in 1998 by a company named OMV Pakistan, is situated in a study area where OMV Pakistan served as the primary operator of the project. PPL and ENI Pakistan joined forces in a joint venture. This gas field stands out as one of the significant gas discoveries in Pakistan.

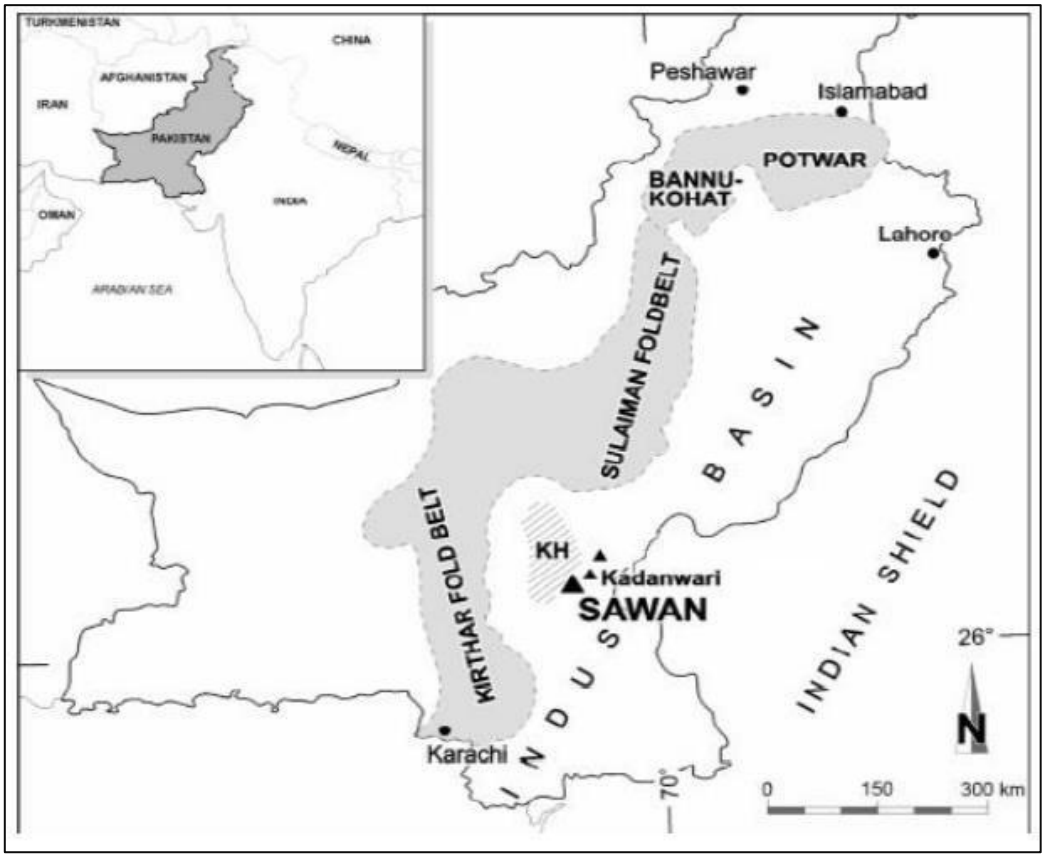

Figure 1.1: Map showing location of Sawan field (after Berger et al., 2009).

Early Cretaceous Lower Goru “C” Interval Sand formation act as a Prolific, which trapped by distally up dip stratigraphy in westward direction along with some Structural features. The charging source of Lower Goru formation is Sembar Formation of Cretaceous age that was confirmed as regional source having rich organic shale in Lower and Middle Indus Basin (Ahmad et al., 2004).

1.3. Exploration History

The Sawan field, a significant gas reservoir located in the Lower Indus Basin, Khairpur District, Southern Pakistan (Late Cretaceous), spans the geographical coordinates between 24° and 28°N Latitude and from 66°E Longitude to the Eastern boundary of Pakistan. Discovered in 1998 by OMV (Pakistan) Exploration, the Lower Goru Formation sediments were identified by OMV (Pakistan), OGDCL (Oil and Gas Development Company Limited), and various other companies. The Southern compartment houses the accessible PSTM 3D seismic cube covering approximately 10^2 km. Within the Sawan field, 15 wells have been drilled, with the central compartments being the primary producing zone, known as the main gas tank (Ibrahim, 2007). Fourteen of these wells contribute 270 million cubic feet/day to Sui Southern Gas Company, marking it as one of the major gas reserves discoveries in Pakistan with a total proven gas reserve of (2-2.5 TCF).

Situated in an extensional tectonic regime revealing horst and graben structures, the potential reservoir in the Sawan field is the Lower Goru, characterized by a shallow marine depositional environment and charged by Shale of Sembar Formation. The Sembar Shale of the Lower Cretaceous serves as the source rock, rich in shales, and is sealed by the Upper Goru Formation, composed of very fine to fine and silty sandstones. Sawan-1, the initial exploration well, targeted a methane-rich gas column, accounting for 10% of the original evaluation. Subsequently, Sawan-2 and Sawan-3, explored after 7 to 8 years, were appraisal wells. The establishment of the Sawan Central Processing Plant (CPP) in 2003-2004 significantly contributed to production, yielding 1.4 TCL (Trillion Cubic Feet). The Lower Goru Formation, a vital contributor, constitutes 14% of the discovered hydrocarbon reserves in Pakistan (Jamil et al., 2012). As the study

area presents challenges in low production, further research on the Lower Goru Formation is imperative, aiming to resolve these issues (Ashraf et al., 2021).

The primary objective of this study is to map the productive sands of the Lower Goru Formation within the Sawan field.

1.4. Data Set:

The following data sets (seismic and well) were used for research in the study area; they were acquired by Land Mark Resources (LMKR) with permission from the Directorate General of Petroleum Concessions (DGPC).

- Customized 3D Seismic Data Cube (10*10 km^2)
- Digital Well Logs (LAS files of three wells)
- Navigation Files
- Seismic Header Files
- Formation Tops

1.4.1. Seismic Data:

The OMV-Sawan-3D-1999, Seismic Block (10*10 km^2) that has been used for studying the area, marking horizons and identification of stratigraphic or structural geometries. The 3D Seismic Data Cube is formed of In-Lines and Cross Lines. The In-Lines ranges from 718 to 858. The Cross Lines ranges from 874 to 1004.

1.4.2. Well Data:

Three Wells (Sawan-01, Sawan-07 & Sawan-08), have been used for research purposes in Sawan area. Sawan-01 is used to generate Synthetic Seismogram and for well to seismic tie.

Table 1.1: Well data used in reservoir characterization.

WELL NAME	LATITUDE	LONGITUDE	STATUS	CLASS	TD(M)
SAWAN-01	26.991828	68.906992	GAS	Exploratory	3587
SAWAN-07	26.999283	68.923317	GAS	Development	3400
SAWAN-08	27.009156	68.933394	GAS	Development	3430

1.5 Software Used

- Petrel Software
- Geographix Software
- HRS software.

1.6 Literature review

One of the widely used methods for characterization of the reservoir is seismic inversion. Seismic inversion aids in combining the seismic and well data for predicting the characteristics of reservoir (Wang et al., 2017). Reservoir characterization of mixed facies and tight sands in Central Indus Basin Pakistan was performed by (Toqeer et al., 2021) . By making use of seismic data and well log data as an input reservoir modeling, model based seismic inversion and post stack seismic inversion was done along with generation of cross plots of effective porosity and acoustic impedance. By making use of seismic attributes interpreters are able to extract more information from original seismic data. By using 2D seismic data as input and by performing seismic attribute analysis, Goru Clastic of Indus Basin Pakistan were evaluated by (Tayyab et al., 2017).

2D and 3D seismic data was used for analyzing the reservoir potential of Southern Indus Basin, Pakistan by performing model based and Stochastic inversion and by making cross plots of neutron and density logs (Asim et al., 2016).

By using 3D post stack seismic data as input dataset, spectral decomposition and coherence attribute were used by (Tayyab et al., 2017) in order to find fluvial sand reservoirs Southwest Pakistan's Indus Basin. Petrophysical analysis of Lower Goru Formation and reservoir quality analysis was performed by using well log data of number of wells including Mehrab-1, Kadanwari-4, Gajwaro-1, Kadanwari-3 and Nara- (Qadri et al., 2019).

Artificial neural network and seismic inversion analysis were used (Qiang et al., 2020) to predict the reservoir quality of the Sawan Gas field, Pakistan. During this research cross plots of porosity and acoustic impedance were created and support vector machine was used (Qiang et al., 2020).

1.7 Purpose of research

Previous studies used seismic interpretation, petrophysical analysis, seismic attributes, and inversion to assess the hydrocarbon potential of various areas in the Southern Indus Basin. However, there is no work on making use of machine learning to identify the thin packages of sand in Lower Goru Formation of Sawan Gas Field. Based on the above literature review it was revealed that there is no work on making use of machine learning to identify the thin packages of sand in the Lower Goru Formation of Sawan Gas Field. Along with that no research has been previously done for calculation of geomechanical parameters of wells in Sawan Gas Field.

So, my research will focus on thin bed detection by seismic attributes. Cross plot porosity and permeability prediction by making use of Machine Learning and neural network, computation, and validation of shear sonic using machine learning, geomechanical parameters calculation, and creation of cross plots such as Vp, Vs, density etc.

1.8. Base Map:

The Base Map serves as the fundamental representation of primary data, illustrating the orientation of 3D In-Line and Crosslines, and indicating the position of wells with Projected Coordinates (X, Y). In this visualization, In-Lines are oriented from the Northwest (N-W) to the Southeast (S-E), while Crosslines are directed from the Northeast (N-E) to the Southwest (S-W). The accompanying figure showcases the 3D Survey of the Sawan Gas Field, specifically utilized for research purposes. This comprehensive depiction offers a

spatial understanding of the survey layout and aids in the interpretation of the field's geological and geophysical characteristics.

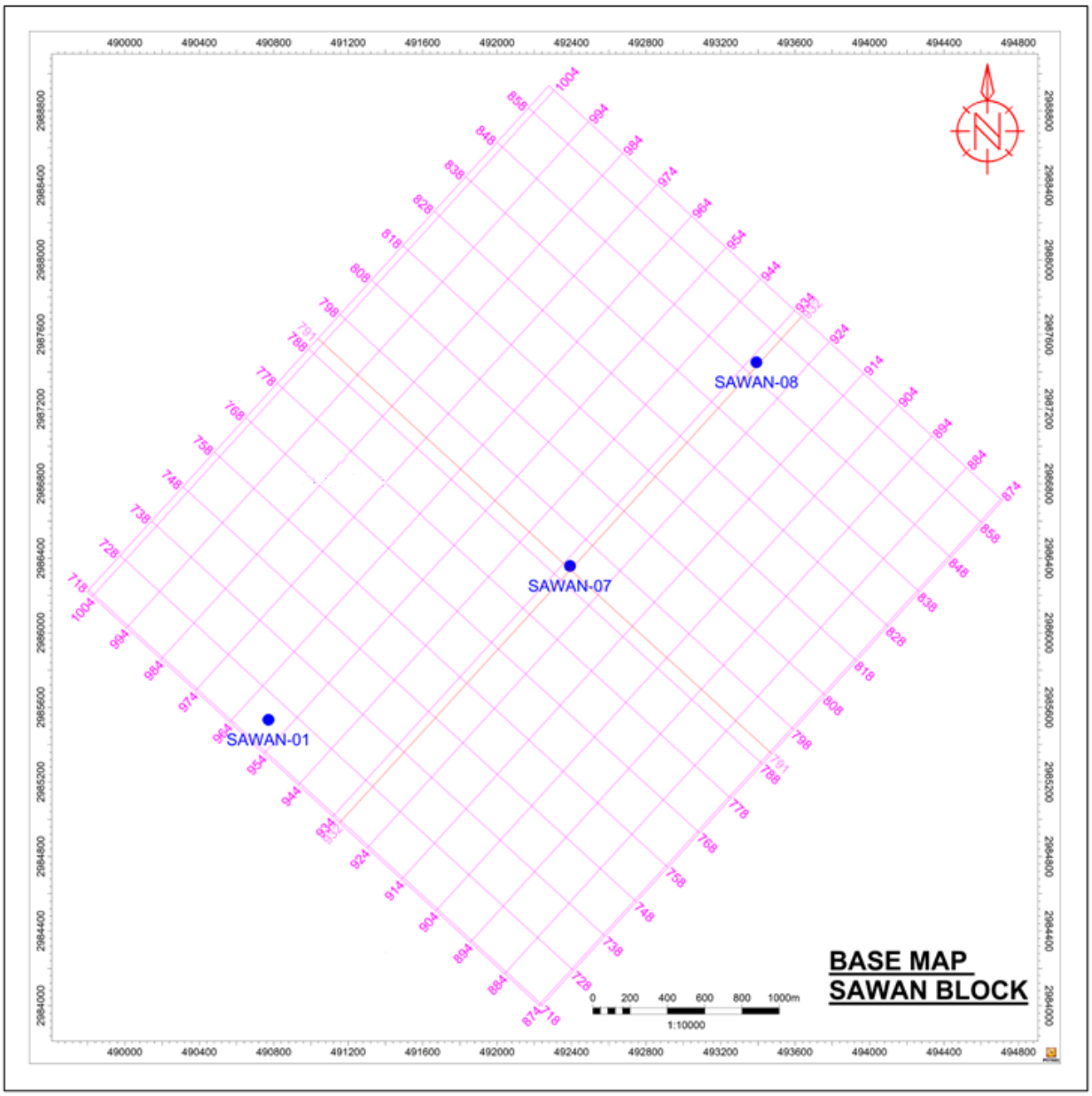

Figure 1.2 Base map of Sawan Gas field.

1.9. Objectives of the Study:

The primary goal of the study is to better evaluate the C-Interval Sand of the Lower Goru formation using various quantitative approaches.

- Analyzing detailed 3D seismic interpretation to find out subsurface structures favorable for hydrocarbon accumulation.
- Examining rock properties and fluid content for essential reservoir insights using petrophysical analysis.
- Characterizing reservoir properties on a larger scale using inversion techniques.
- Utilizing machine learning techniques for the estimation of petrophysical parameters in reservoir formations.
- Using rock physics models for the evaluation of low-impedance sand packages.

1.10. Methodology

The research commenced with a comprehensive review of the geological and tectonic aspects of the study area. One-dimensional (1D) forward modeling, specifically synthetic seismogram generation using seismic and well data, was employed to establish optimal correlation between synthetic and actual seismic data at well locations, accurately marking horizon positions. Subsurface geometry was then depicted through two-dimensional time and depth contour maps using Kingdom 8.6 Software.

Petrophysical analysis utilized high-resolution well log data, displaying logs such as Spontaneous Potential (SP), Gamma Ray (GR), Caliper Log (CALI), Deep Laterolog, Shallow Laterolog, and Micro Spherical focused log. Porosity tracks incorporated Sonic log (DT), Density log (RHOB), Neutron log (NPHI), enabling the determination of Shale Volume (Vsh) and various porosity measures like Density Porosity (DPHI), Total Porosity (PHIT), and Effective Porosity (PHIE), along with water and hydrocarbon saturation.

The research culminated in Seismic Post Stack inversion, characterizing the reservoir by converting seismic data into quantitative properties such as impedance. Model-based inversion results to be computed, including the evaluation of porosity results. Additionally, geostatistical methods were applied for porosity estimation in inversion types, facilitating a comparative analysis. Despite inherent risks and uncertainties, these methodologies prove invaluable for reservoir management and development.

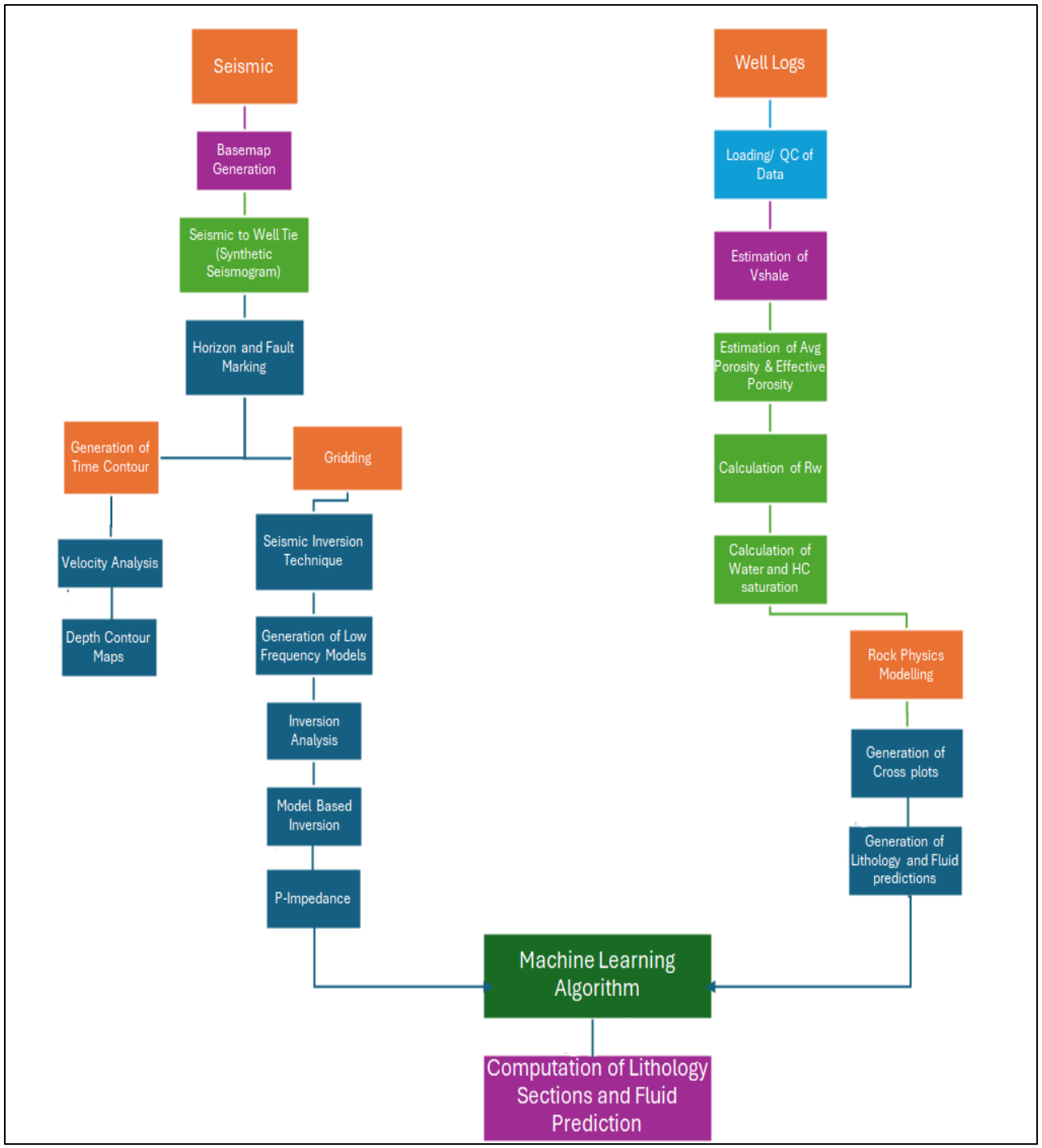

Figure 1.3 Methodology and the implementations strategy adopted for the execution of this dissertation.

CHAPTER 02

GEOLOGY OF STUDY AREA

2.1. Introduction

The geology of the study area is a crucial factor in seismic and stratigraphic interpretation, as highlighted by Bacon et al. (2003). Geophysicists need a profound understanding of both local and regional geology for accurate seismic interpretation, as emphasized by Badley (1987). Geology describes origin, mode of deformation, structural style, and depositional environment. Therefore, the interpreter must have the knowledge of geology of the study area to overcome the complexities during interpretation.

2.2. Geological Settings

Based on structural development, stratigraphic style, and sedimentary history, the Indus Basin is categorized into three major parts:

- Upper Indus Basin
- Central Indus Basin
- Lower Indus Basin

Moreover, Jacobabad, Khairpur, and Mari Khandkot are identified as elevated areas within the Indus Basin, located in the central and southern parts. Historically, these high areas have played a significant role in the discovery of major hydrocarbon deposits, providing effective trapping mechanisms through their structural and stratigraphic styles. Combined traps, conducive to migration pathways, reservoir charge timing, and hydrocarbon accumulation, have been identified as particularly favorable (Kazmi and Jan, 1997).

The Sawan area, situated in the Lower Indus Basin within the Khairpur district of Sindh Province, Pakistan, is renowned for its gas production. Referred to as the Sawan Gas Field, it is in the Thar Desert. The boundaries of the Indus Basin are delineated by Indian cratons to the East, the Kohat Peshawar Plateau to the North, and the fold and thrust belts of Sulaiman and Kirthar ranges to the West. The research area lies in the North-West direction, encompassing the Khairpur high characterized by a notably high geothermal gradient. Khairpur High, being a basement high, is enclosed by sands and carbonates in the eastern portion near Khairpur and Sukkur areas (Azeem et al., 2016).

Figure 2.1 Tectonic Map showing Sawan Area illustrating major tectonic features in the vicinity (Rehman et al., 2013).

2.3. Tectonic Settings

The unveiling of the Lower Goru primarily occurred on the Jacobabad High and Mari High within the Lower and Central Indus Basin, known for their structural

characteristics. These structural highs serve as migration pathways and are conducive to hydrocarbon accumulation. Three tectonic episodes associated with post-rifting have shaped the structural configuration. These are as: Cretaceous uplifting and deterioration, basement embedded NNW-SSE aligned wrench faults and late tertiary to current uplifting of Jacobabad and Khairpur highs (Ahmad et al., 2004).

The initial episode is the Cretaceous uplifting and deterioration occurred near the K-T boundary, marked by Late Cretaceous Uplifting. The reduction of Ranikot clastic rocks around the Paleo high and their subsequent increase confirmed this event. The second episode resulted from the collision of the Indian and Eurasian plates. The Indian plate's anti-clockwise rotation led to wrench faulting, particularly impactful to the east of the Sawan area. These faults, shearing the entire Cretaceous section, exhibit a flower-like pattern with varying properties and terminate against the Tertiary unconformity. They form en-echelon faults with minor throw. The Wrench faults shear the whole Cretaceous part and their property varies from one fault to many en-echelon faults. These faults discontinue at odds with tertiary unconformity. They make flower-like pattern having minor throw. The last episode is from late tertiary to current uplifting of Khairpur/Jaccobabad high. Due to this uplifting, Lower Goru reservoir quality Sand converts to structurally deep areas, whereas non reservoir quality distal parts are oriented up dip to form the traps (Berger et al., 2009). In this stage, structural and stratigraphic traps formed and Paleo high, secondary hydrocarbon migration and reservoir charge also took place (Ahmad et al., 2004).

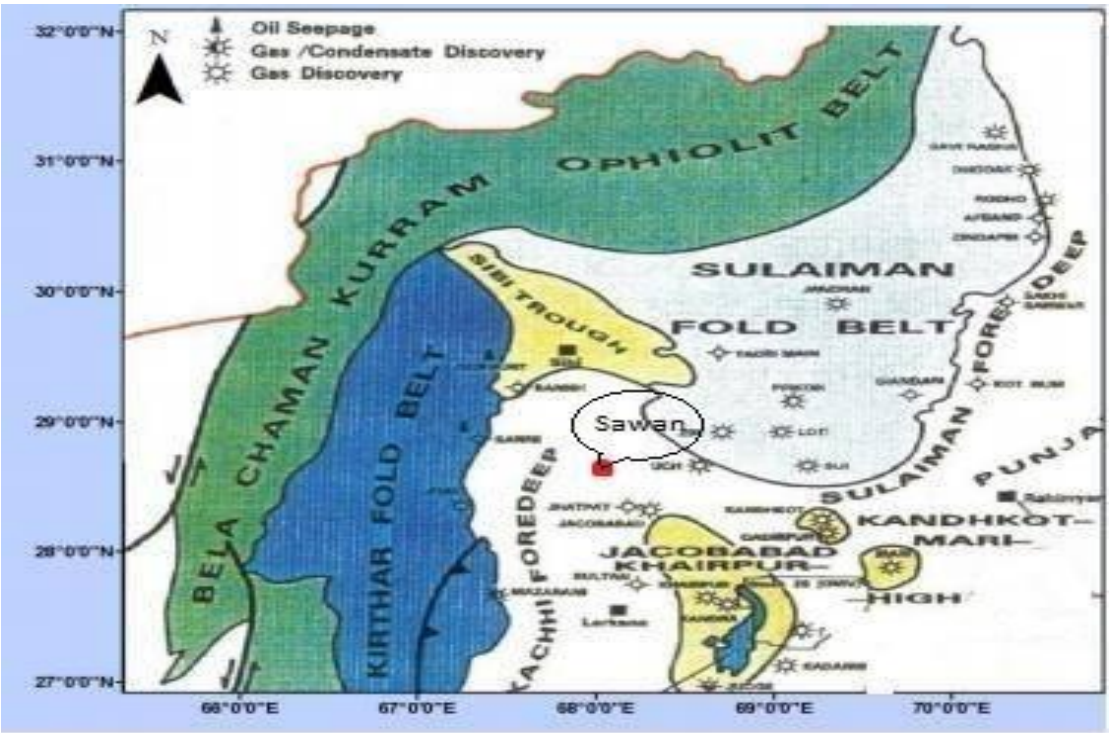

Figure 2.2. Tectonic Map of Lower Indus Basin (Rehman et al,2013)

The figure illustrates significant discoveries in the Lower Indus Basin, including the location of the study area, such as the Sawan Gas Field. Situated in the Southern Indus Basin of Pakistan, Sawan Gas Field spans between 24° and 28°N latitude and from 66°E longitude to the eastern boundary of Pakistan (Zaigham and Mallick, 2000). The geological influences on this region are primarily attributed to the movement between the Afghan Craton and the Indian Plate from the northwest, as well as the convergence between the Afghan Craton and the Arabian Plate. The dominant geological impressions stem from the collisions between the Indian and Eurasian plates. Subsurface declarations manifest in the form of normal faulting, horst and graben structures, attributed to the West rift margin, extending below the base of Paleocene within the Cretaceous in the Lower Indus Basin (Shuaib, 1982). The West Indus Plain, shaped by normal faulting, serves as a significant migration path for hydrocarbons from the fundamental Shaly source sequence. Noteworthy structures observed in the Sawan area include dome structures and rifting, with surface expressions seen in Sibbi-Jacobabad, Khairpur, and Mari-Kandkot highs (Kadri, 1995).

2.4. Stratigraphy of Lower Indus Basin

The stratigraphic sequence in the Sawan area exhibits variation from East to West. Pre-Cambrian basement rocks are prominent in the southeastern portion of the basin, while towards the West, the sedimentary sequence thickens. The Jacobabad–Khairpur high encompasses Tertiary, Mesozoic, and Quaternary lithologies, with a key unconformity occurring between the base Permian and base Tertiary, indicating deposition during the early rifting stage. The Sui Main Limestone, settled on a shallow water carbonate, is considered a favorable hydrocarbon reservoir. The Goru Formation, lithologically divided into Lower Goru and Upper Goru, is a focus in this study, particularly the Lower Goru. Comprising medium to coarse-grain sandstones in a shallow marine environment, it overlays the Sembar Formation, a crucial source stratum in the region. The Lower Goru is further categorized into five divisions, with alternating sand-shale layers forming potential reservoirs. These sand-bearing sequences, deposited in deltaic marine, strand plain, and barrier bar shoreface to offshore settings, are considered excellent reservoirs in the lower part of the Indus Basin.

The A, B, C, and D intervals are the lithostratigraphic units of Lower Goru; the sands from the B and C intervals could be reservoirs in the Sawan region. Black to grey shale makes up the majority of the Goru Formation's lower portion, although substantial sand deposits may be found in its top portion. This sandstone is notable for its reservoir properties in the Sawan region and other regions of the Southern Indus Basin. The upper portion of the Lower Goru is dominated by shale, which serves as a barrier between the reservoir sand intervals below. The upper shale unit is known as Upper Goru, whilst the lower sandy portion of the formation is known as Lower Goru.

The Goru Formation was deposited in a relatively deep marine environment, with the Lower Goru potentially representing barriers to deltaic environments (Munir et al., 2011). Cretaceous rock which over lie the Goru Formation is thin bedded argillaceous Parh Limestone of light grey to white color. These are overlain by siliclastic Ranikot Formation of Paleocene (Munir et al., 2011).

Table 2.1: Generalized stratigraphy of the Lower Indus Basin (Kadri, 1995).

AGE	FORMATION		LITHOLOGY	SYMBOL	PLAY SYSTEM
PLEISTOCENE	SIWALIK		SANDSTONE & CLASTIC CLAY		
EOCENE	KIRTHAR		SHALE & MARL		
	LAKI		LIMESTONE & SANDSTONE		
PALEOCENE	RANIKOT		LIMESTONE & SANDSTONE		
	KHADRO		SANDSTONE, SHALE & LIMESTONE		
CRETACEOUS	PAB		SANDSTONE		
	MUGHAL KOT		MUDSTONE & SHALE		
	PARH		LIMESTONE,SHALE & MARL		
	UPPER GORU		LIMESTONE & SHALE		SEAL ROCKS
			UPPER GORU SHALE		
	LOWER GORU	UPPER SAND	A SAND		RESEVOIR ROCKS
			TURK SHALE		
			B SAND		
			BADIN SHALE		
			C SAND		
			JHOL SHALE		
			D SAND		
			UPPER SHALE		
		MIDDLE SAND	MIDDLE SAND		
			LOWER SHALE		
		BASAL SAND	UPPER BASAL SAND		
			TALHAR SHALE		
			LOWER BASAL SAND		
	SEMBAR		SEMBAR SAND & BLACK SHALE		SOURCE ROCKS
JURASSIC	CHILTAN		LIMESTONE & SANDSTONE		

2.5. Petroleum Play

In the petroleum system of the Sawan area, the source, reservoir, and cap/seal rocks, with the migration of hydrocarbons playing a pivotal role. The drilling and logging results indicate the presence of a complete petroleum system of Cretaceous age in the Sawan area.

- Sembar Formation
- Goru Formation
- Chiltan Formation

2.5.1 Source Rock:

Based on previous study, it has been considered that Sembar Formation and Goru Formation serve as the major source rocks in the Central and Lower Indus Basin. In the Western part of the Southern Indus Basin, secondary source strata consist of transgressive marine shales of Upper Paleocene age, which are buried (Zaigham and Mallick, 2000). During the early Cretaceous age, the Sembar Formation's depositional environment was shallow marine. It is characterized by black shale, sandstone, siltstone, and nodular argillaceous limestone. The primary organic material in the Sembar Formation is Type-III Kerogen, making it highly promising for gas production (Wandrey et al., 2004).

2.5.2 Reservoir Rock:

The Lower Goru Formation, a key reservoir rock in the Sawan field, is characterized by intercalations of sand-shale layers. Within the lower portion of the Cretaceous Goru Formation, there are high-quality reservoir sandstones, categorized as A, B, C, and D. Among these, the C-Interval Sand, from these alternating packages, stands out as the most prolific reservoir in the Sawan field. In the study area's reservoir strata, particularly the C-Sand Interval, thin shale sequences interbedded with sandstones contribute to high heterogeneity. The variability in sediment texture, ranging from very fine to coarse sands, poses challenges in spatial facies interpretation (Ashraf et al., 2020). The potential for hydrocarbons in this area is extensive, and a comprehensive understanding of the dispersal of sand-shale intercalations is crucial (Ashraf et al., 2019). Seismic stratigraphy and core sedimentology studies suggest that the C-Interval Sand represents a Lowstand Shelf Edge Delta system (Ahmad et al., 2004; Afzal et al., 2009; Munir et al., 2011). The porosity of the C-Interval Sand reservoir ranges from 6-25%, and permeability ranges from 1-2000mD. The Lower Goru Formation spans various environments, including barrier bars, lower shorefaces, and deltaic settings (Shah, 2009).

2.5.3 Trap and Seal:

In the Lower Indus Basin, multiple sealing intervals, including the substantial Ghazij Shales, Lower Goru Shale intervals, and the Ranikot Shale unit, are present (Shah, 2009). The thick shale bed of the Upper Goru from the Late Cretaceous acts as a seal for C-Sands reserves in the Lower Indus Basin. Structural-cum-stratigraphic traps have been identified in

the Sawan area, developed during the third phase of tectonic events known as the inversion. During migration, shale layers terminate (pinchout) against prograding C-Sand wedges in the westward direction, creating a stratigraphic trap. Additionally, a northwest to southeast trending wrench fault contributes to establishing a combined trap in the study area. The Lower Goru formation is regionally capped by thick transgressive shale, and the intraformational shale within the Lower Goru also serves as a seal phase (Ahmad et al., 2004; Berger et al., 2009).

CHAPTER 3

SEISMIC DATA INTERPRETATION

Seismic interpretation's primary goal is to precisely characterize the lithology and subterranean geological formations. Rocks that contain hydrocarbons can be distinguished from rocks that do not by using seismic data analysis (Ahmad et al., 2021). Seismic interpretation becomes quite challenging in areas of complex tectonics. Therefore, in such cases in order to carry out accurate interpretation it is necessary to make correct observations in both subsurface as well as surface data (Zamora et al., 2022).

The seismic record consists of two essential elements. The initial aspect involves the timing of the arrival of any reflection (or refraction) from a geological boundary, while the second is the shape of the reflection (Bouvier et al., 1991). The lithology and fluid content of the seismic reflector being studied are frequently deduced from the seismic data (Bouvier et al., 1991). Seismic interpretation is divided into structural interpretation and stratigraphic interpretation. The goal of structural seismic interpretation is to create structural maps of the subsurface using the observed three-dimensional configuration of the arrival times. A model of cyclic episodes of deposition relates to the pattern of reflection observed through seismic sequence stratigraphic interpretation (Bouvier et al., 1991).

Digital representations of seismic data, recorded by each channel of the recording instrument, are expressed as time series. Processing algorithms are formulated and utilized for either individual single-channel time series or multichannel time series (Yilmaz, 2001). The Fourier transform forms the fundamental basis for a substantial portion of the digital signal processing methods used in the examination of seismic data. Beyond the sections that address one- and two-dimensional Fourier transforms and their real-world applications, the

core principles of signal processing also include a dedicated section that explores a diverse compilation of seismic data recorded from various regions worldwide (Yilmaz, 2001). Through reference to field data examples, interpreters analyze the type of seismic signals, including primary reflections from layer boundaries and various forms of noise, both random and coherent (Yilmaz, 2001).

3.1 Seismic Interpretation's Workflow

To perform Seismic Interpretation, the following workflow is adopted.

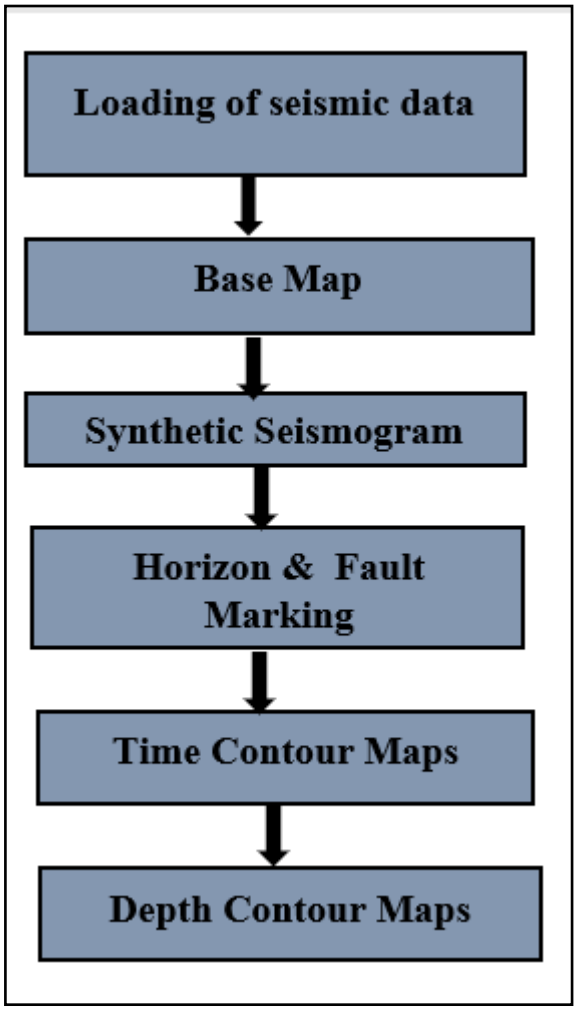

Figure 3.1 Workflow adopted for seismic interpretation adopted during research.

3.1.1 Loading of Seismic Data

A 3D seismic data cube in SEGY format of Sawan Gas Field area was provided by DGPC. The data was loaded into Petrel software by using the SEG Y headers for cross line and inline loading.

3.1.2 Base Map

After the completion of the seismic data loading, the base map of the provided cube is generated. The base map displays how the overall grid is oriented. There are two types of lines in a 3D cube: in lines and cross lines. The cross line lies between the numbers 390 and 540, as illustrated in Figure 3.2, while the inline runs from 1310 to 1470. The Sawan-01 is located on inline 1459 and cross line 520, Sawan-07 is located on inline 1407 and crossline 420.

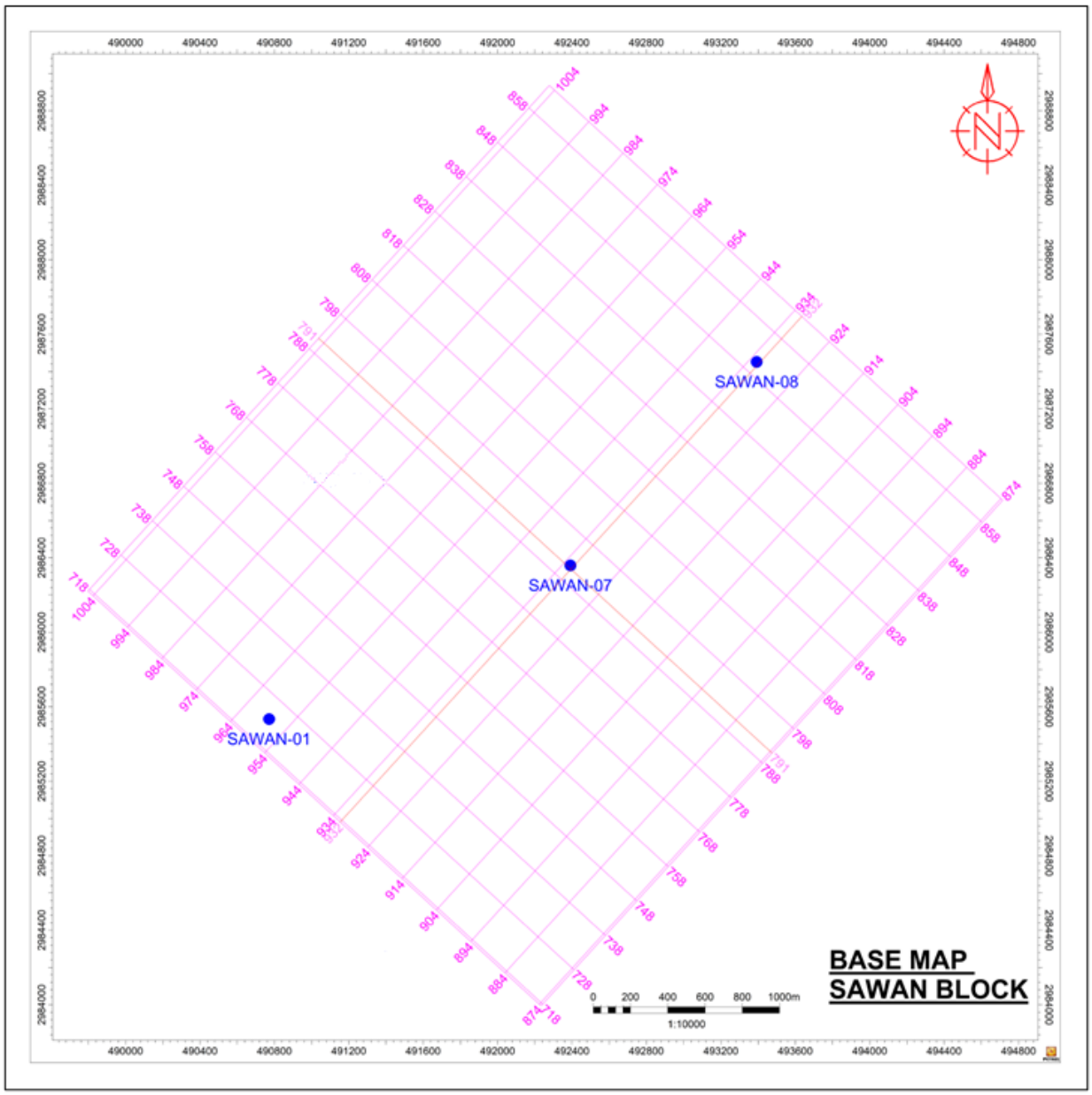

Figure 3.2 Base map of the study area showing the distribution of in lines and crossline along with type of well.

3.1.3 Synthetic Seismogram

Synthetic seismogram serves as a "tie" in hydrocarbon exploration between seismic reflection data collected at the same location and changes in rock characteristics observed in a borehole (Helmberger et al., 1989). The wavelet derived from seismic data is convolved with the reflectivity derived from digitized acoustic and density logs to generate the synthetic

seismogram. Interpretations of data can be improved by comparing the marker beds or other correlation points noted on the well logs with the notable reflections on the seismic section (Helmberger et al., 1989).

Synthetic seismogram's ability to match depends on a variety of parameters and these are as follows:

- How well seismic data is processed?
- Quality of the well logs
- Ability to extract a representative wavelet from seismic data (Helmberger et al., 1989).

Synthetic seismogram is essential to make a correlation between seismic data and the geological data which is in form of well logs. To make a synthetic seismogram following elements are needed:

- Sonic log
- Time Depth Charts
- Density log
- Reflection coefficient (RC)
- Acoustic Impedance(Z)
- Wavelet

Once the synthetic seismogram is created its signature and the original seismic data's signatures are compared. From the adjacent seismic trace in the vicinity of the wells, a seismic trace was taken for each well. This extracted trace represented the original seismic data to be used in the synthetic matching. After that the signature of the synthetic seismogram and seismic data were compared. Shift and stretch were then used to make alterations and once the nature of seismic data and synthetic seismogram matched the well to seismic tie was completed (Kelly et al., 1976).

A seismogram is necessary for a well-to-seismic tie. Therefore, density log and sonic log from the Sawan 01, Sawan 07 and Sawan 08 along with gamma ray log is also used as a references log.

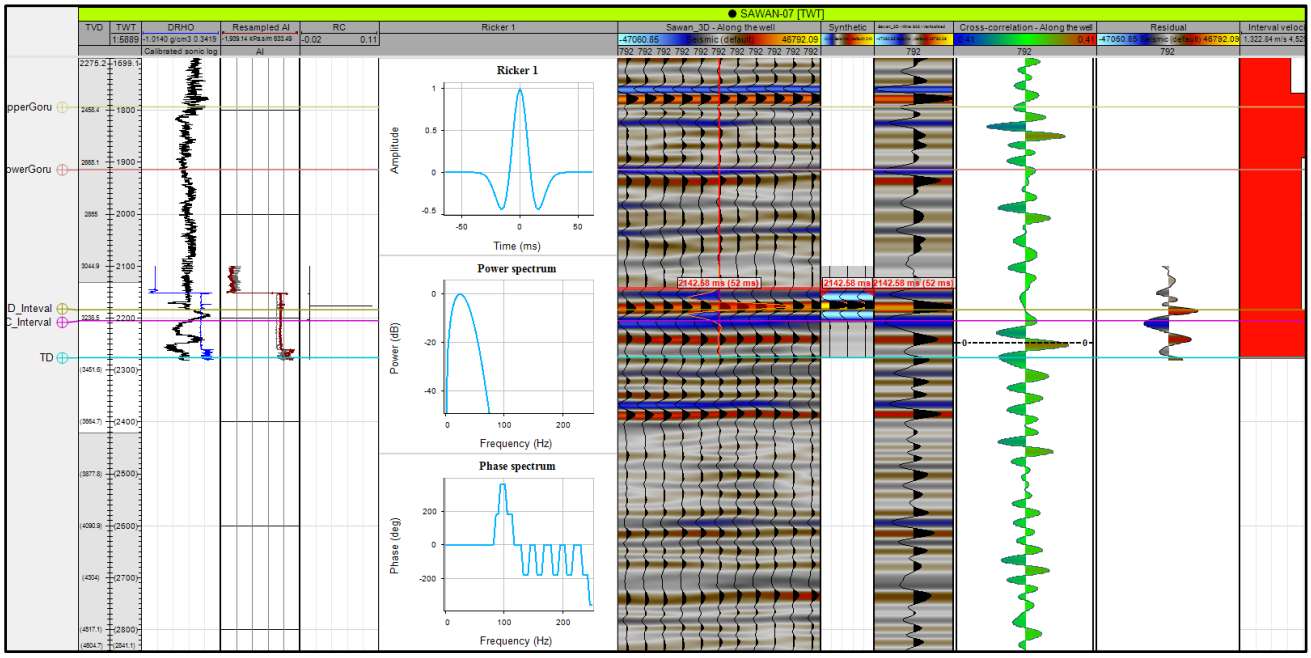

Figure 3.3 Synthetic Seismogram of Sawan-07

3.1.4 Horizon and fault marking

Interpreting and marking various horizons on seismic data is the first and most fundamental step in seismic interpretation. Understanding the structure and stratigraphy of the research area is necessary for accurate interpretation. Two horizons are interpreted. namely C-Interval and D-Interval. These are the sand intervals of Lower Goru Formation. Identifying the pattern of the faults becomes quite easy when one knows about the stress regimes that exist in the study area. Usually, the reverse faults are associated with compressional tectonics regimes and normal faults are dominant in the extensional tectonics. The study area Sawan area lies in the extensional tectonic regime and thus there is presence of normal faults (Freeman et al., 1991).

The research area's fault extension is defined by fault correlation, which also delineates dip directions and specifies the throw which is actually vertical component of the separation and heave which is the horizonal component of slip. The fault correlation aids in defining the fault's network. On seismic data the faults are interpreted when there appears a certain breakage on the seismic section (Freeman et al., 1991).

Interpreted sections:

On the seismic section two horizons C-interval and B-interval were marked both lie within 2 to 5 seconds.

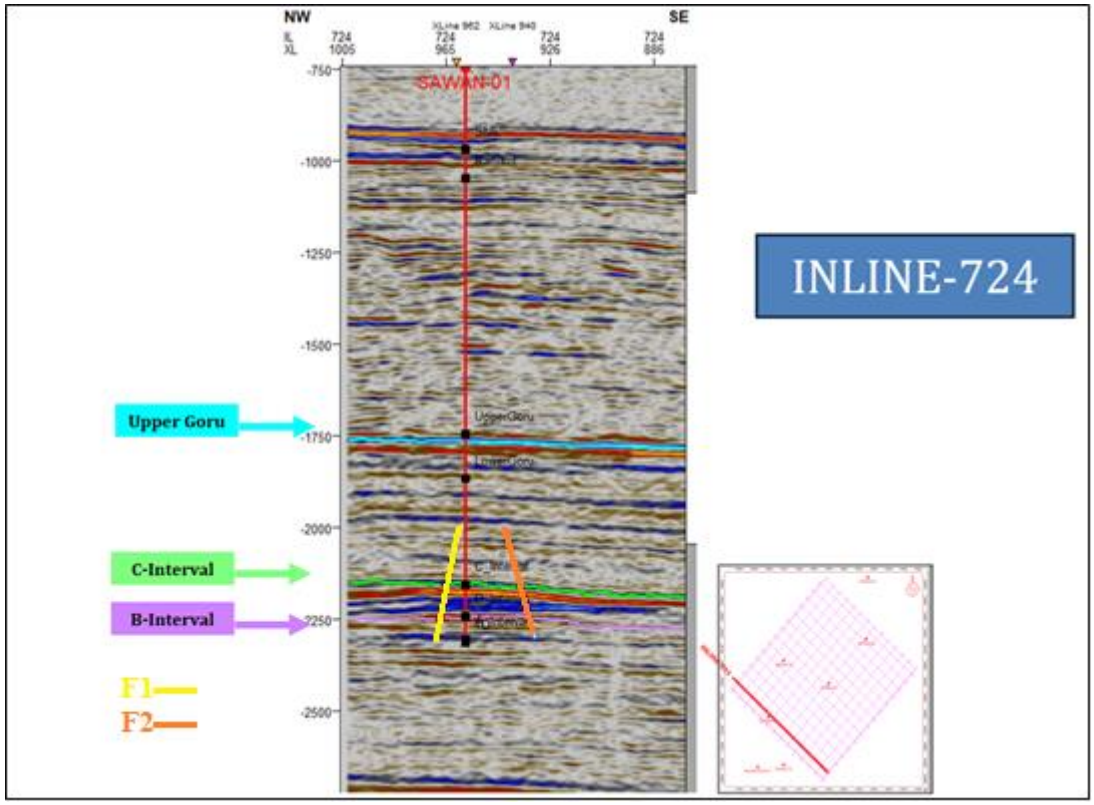

Figure 3.4 Seismic section along with horizons of interest and faults at inline-724.

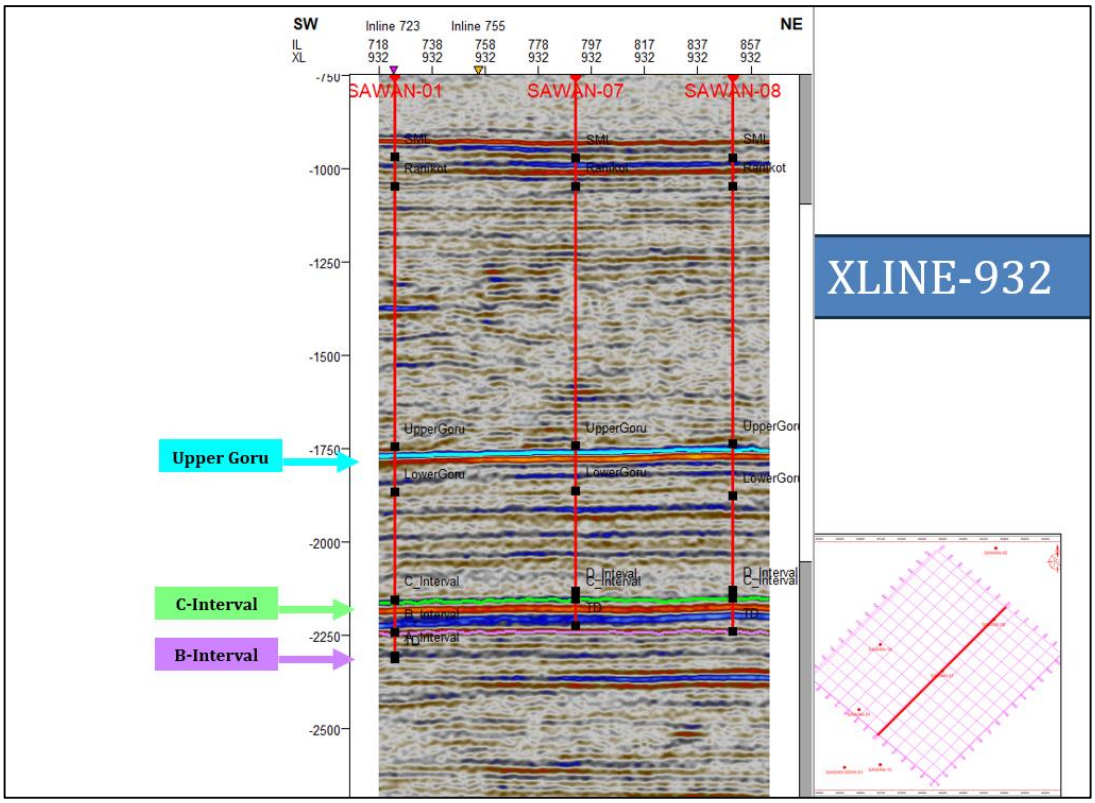

Figure 3.5 Seismic section of Xline-932 with well location of Sawan- 01, Sawan-07 and Sawan-08 along with the Upper Goru formation and C and B Intervals.

3.1.5 Preparation of Contour Maps

The creation of contour maps is the last stage of interpretation. Lines that connect points of the same depth, height, or time are called contours.

TWT contour maps are initially created in the seismic interpretation, followed by depth contour maps. Seismic maps are another name for contour maps. The seismic map is typically the end result of seismic exploration, the one on which the success of the entire exploration's operation depends. A map may be used to highlight specific areas during meetings with the management, but the map itself is crucial for deciding where and if to drill for oil (Caputo & Postpischl, 2010).

Time and depth contour maps are the last stage of seismic interpretation. First, the time contour maps are created because the data is readily available in time and then using the velocity function to transform the time sections into depth section, depth contour maps are

created. Lower Goru's C and B interval's time and depth contour maps are created and explained.

3.1.6 Interpretation of C-interval maps

Based on seismic data seen in the time and depth maps of the C-interval horizon, two faults designated as F1 and F2, are interpreted in the C-interval horizon. Both mentioned faults are normal faults. From the time contour map of the C- interval, the strata on the western side are shallower than those on the eastern side.

The trend of both faults is from NE to SW, and both are dipping towards NW. The nature of faults shows that this area is situated in extensional tectonic regime since these are normal faults. The time contour map of C interval is shown in Figure 3.7. The time ranges for this interval ranges from 2135 to 2205 milliseconds. Time contour values are on the higher side on eastern side of C interval map depicting that the horizon becomes relatively deeper in this area whereas the time contour vales are on smaller side on the western side which shows that in this part the horizon becomes shallow. The contour interval in the map is 5 milliseconds. The horizon is trending from northwest to southeast. The strata exhibit a decreasing time range from east to west. Chances of hydrocarbon accumulation is on the western side as hydrocarbons are present at shallow time.

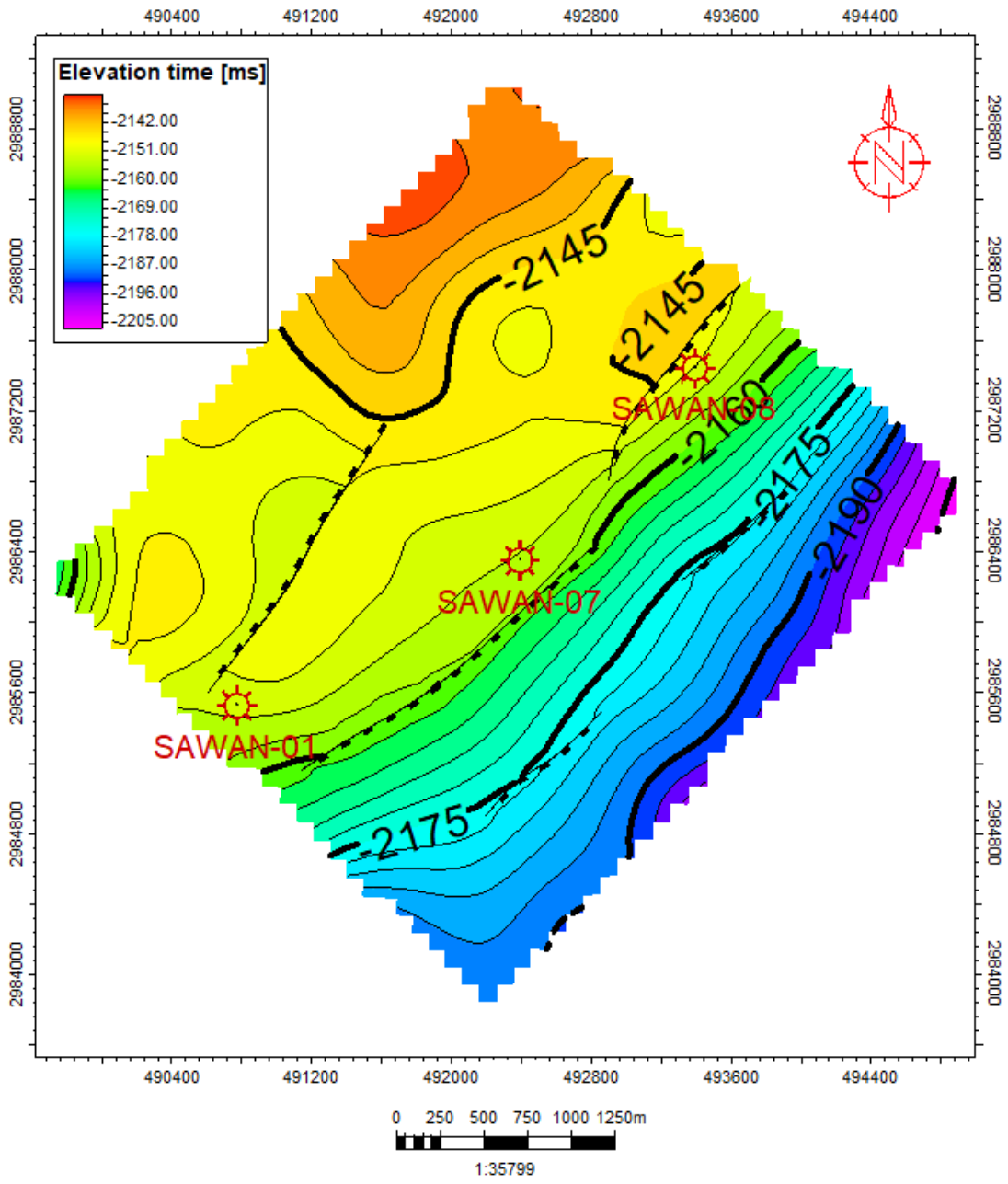

Figure 3.6 The time contour map of C-Sands formation.

As shown in Figure 3.6 depth contour map of C interval ranges from 3170 to 3260 m. The contour interval in this map is 10 m. The unit of the depth contour map is meters. The depth contour map of C-interval shows the same trend as C-interval time contour maps i.e., on the eastern side greater values lie, and the values become higher till 3260 m whereas on

the western side contour values become smaller and decrease to 3170 m. The color bar depicts how the map's contour varies. The strata exhibit a decreasing depth range from east to west. Chances of hydrocarbon accumulation is in western side as hydrocarbons are present at shallow depth.

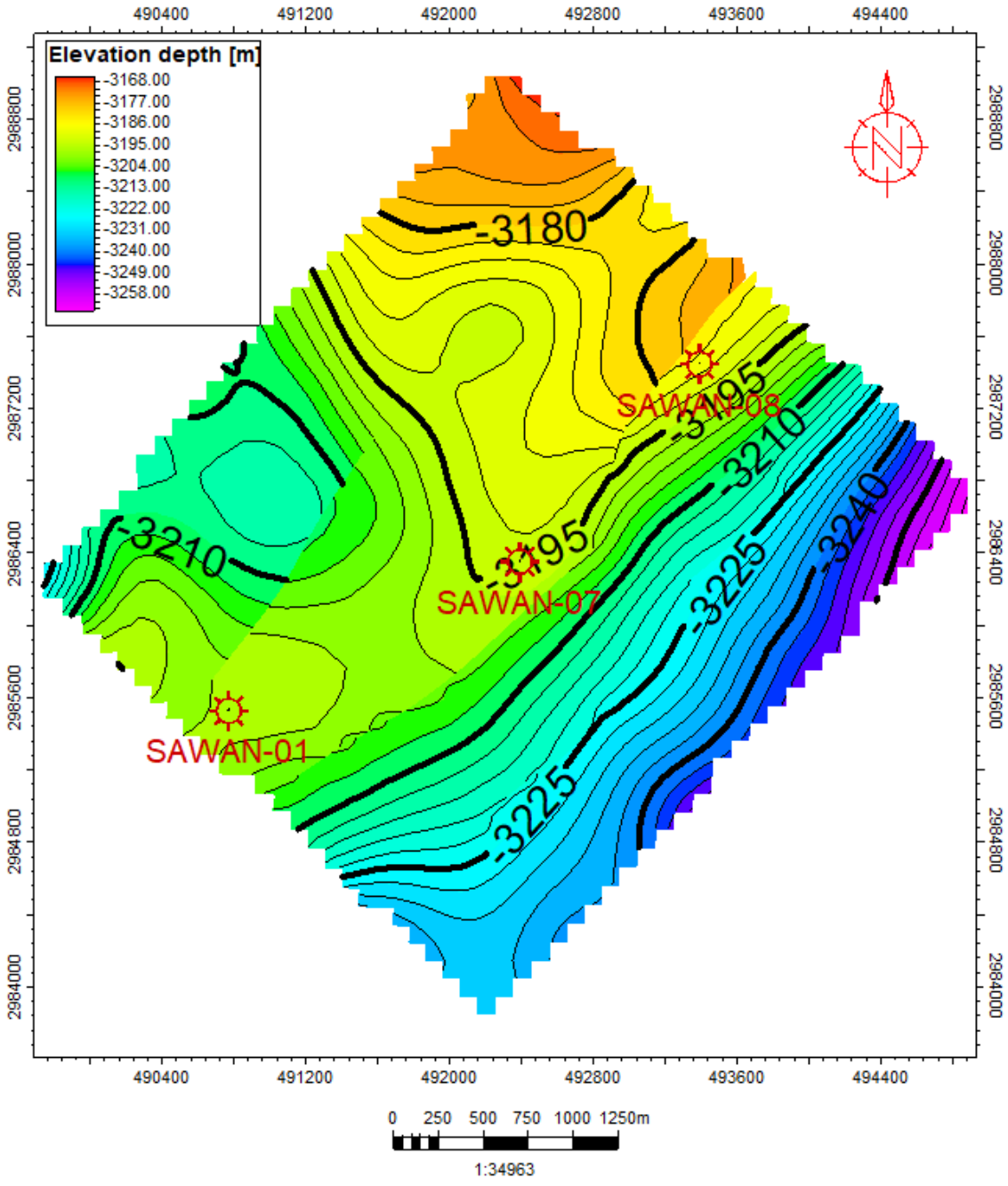

Figure 3.7 Depth contour map of C-Sands.

3.1.7 Interpretation of B-interval maps

The time contour map of B-interval map ranges from 2228 to 2284 milliseconds. The contour interval is 5 milliseconds. Time contour values are highest at the eastern side of B-interval map depicting that the horizon becomes deeper in the eastern side whereas the time contour values are decreasing towards the west showing that at the western side the horizon becomes shallow. From east to west strata is relatively getting shallower i.e., showing less time which might be indicative of hydrocarbons.

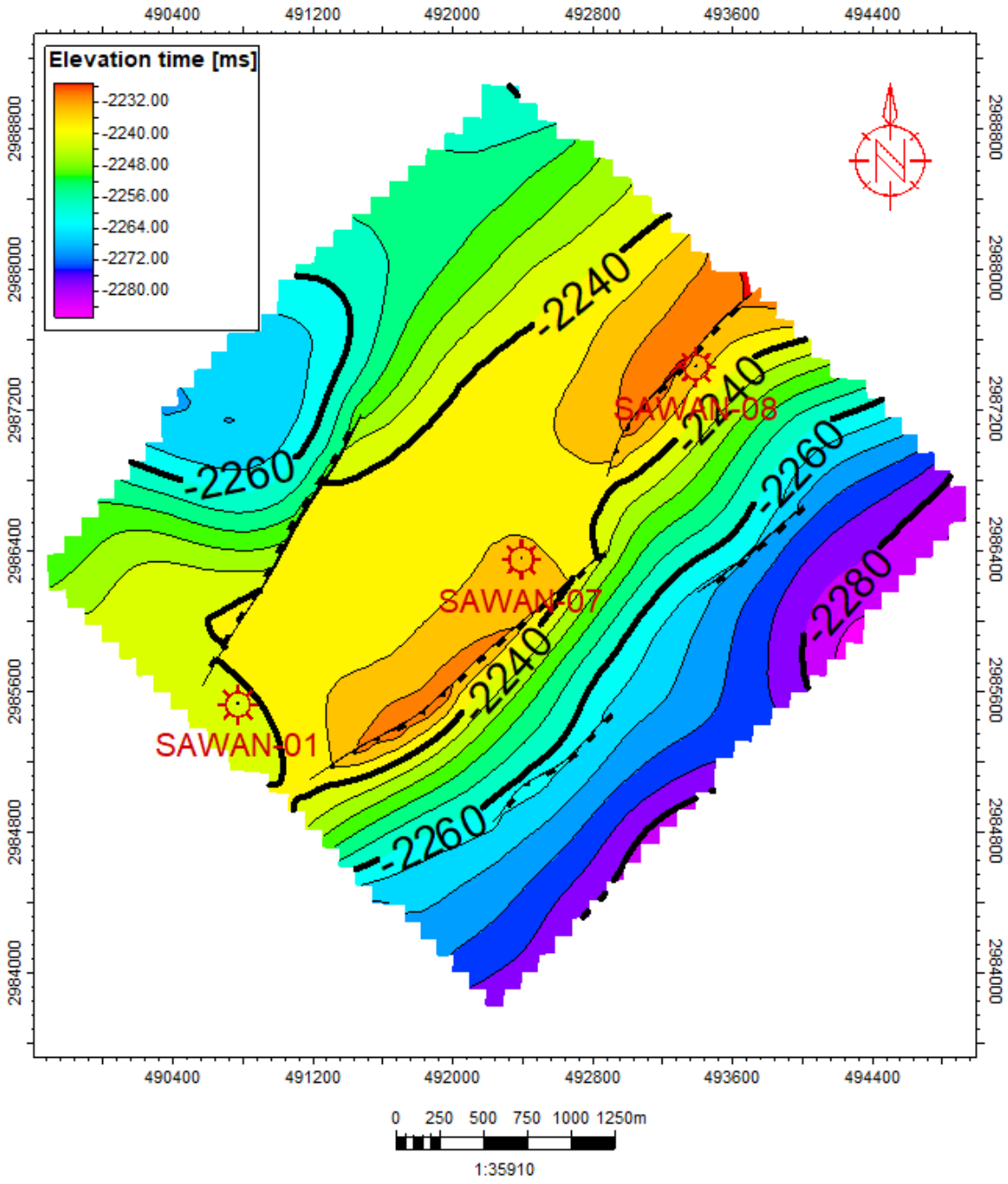

Figure 3.8 The time contour map of B-Sands member of Lower Goru.

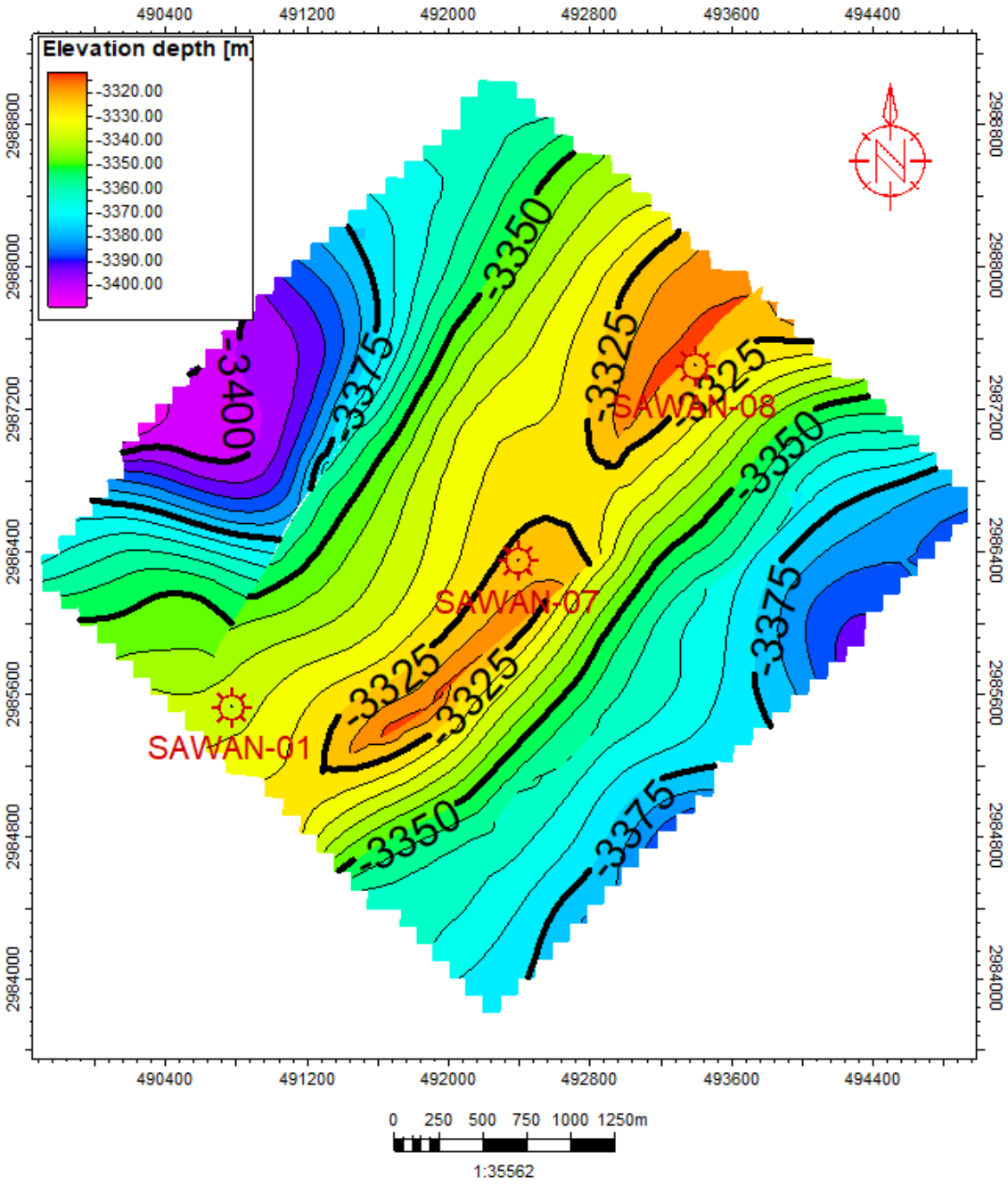

Figure 3.9 Depth contour map of B-Sand that is member of Lower Goru formation.

As shown in Figure 3.10 the depth contour map of B-interval ranges from 3320 to 3400 m. The contour interval in this map is 10 m. The unit of depth contour maps is meters. The depth contour map of B-interval shows the trend that on the eastern greater values lie,

and the values become higher till 3400 m whereas on the western side, contour values become smaller and decrease to 3320 m. The color bar depicts how the map's contours vary.

CHAPTER 04

PETROPHYSICS

4.1 Introduction

Petrophysics is the study of the physical properties of subsurface rocks and their interactions with fluids, encompassing gases, liquid hydrocarbons, and aqueous solutions (Donaldson and Tiab, 2004). This discipline enables the identification of fluid properties within a reservoir and the creation of a geological profile within a borehole (Ali et al., 2014). Petrophysics facilitates the estimation of crucial reservoir properties, including volume of shale, porosity, permeability, lithology of reservoir rock, water saturation, and hydrocarbon saturation. It provides an in-depth understanding of well conditions, aiding in the identification of hydrocarbon-bearing zones (reservoirs) with higher resolution than seismic data. Moreover, well logs offer advantages in the depth domain compared to seismic data in the time domain, yielding more accurate results. Various wireline logs are employed for Well-log analysis, contributing to the identification of reservoir zones of interest (Azeem et al., 2017). Essential logs for this analysis include Density log, Neutron log, Resistivity log, Gamma-Ray log, Sonic log, and Caliper log, which help estimate physical properties like porosity, permeability, and water saturation. This study utilizes well logs to confirm marked horizons, calculate volumetric reserves in the identified zones, and support the overall reservoir characterization process (Rider, 2002).

4.2 Petrophysical Analysis

The Petrophysical analysis has been carried out for the reservoir characterization of the Sawan field. Well logs data of Sawan-01 and Sawan-07 has been utilized to evaluate the different formations.

Steps adopted to perform petrophysical analysis:

- LAS files loading.
- Marking Zone of Interest
- Calculation of Vsh and Vclean
- Porosity Estimation
- Calculation of Rw
- Water Saturation
- Hydrocarbon Saturation

4.3 Lithology identification

Lithology identification involves the use of Gamma-Ray (GR) logs, SP logs, and Caliper logs, with the Gamma-Ray log being a crucial indicator. The GR log measures and identifies the radioactivity within rock formations, primarily arising from the presence of radioactive minerals like Uranium, Potassium, and Thorium. This log is instrumental in distinguishing between shale and clean formations such as sand (Rider, 2012). To separate clean formations from dirty formations, the volume of shale is estimated using the Gamma-Ray log through a linear formula (Donaldson, 2015).

In the linear method, the Index Gamma Ray (IGR) is computed, representing Vsh (volume of shale):

$$\text{Volume of shale} = \frac{(GR)\log - (GR)\min}{(GR)\max - (GR)\min}$$

Where,

GR_{log} = Formation's radioactive values

GR_{max} = Maximum value of gamma ray

GR_{min} = Minimum value of gamma ray

Index Gamma Ray (IGR), give us maximum volume of shale, and we must find minimum volume of shale by non-linear method.

Non-Linear Method:

In the non-linear method, various formulas, including Stabier, Larinov, and Clavier, are employed to calculate the minimum volume of shale. Among these formulas, Stabier is often chosen as it provides the minimum volume of shale.

- **Stabier:** (Most preferable)

  $Vsh = \frac{\text{IGR}}{3-2\,\text{IGR}}$,

  where, IGR= Index Gamma Ray, Vsh is Volume of Shale

- **Larinov:** (Used for Older rocks)

  $Vsh=0.33(2^{2\,\text{IGR}} - 1)$

- **Clavier:**

  $Vsh=1.7-(3.38-(IGR+0.7)^2)^{0.5}$

Volume of Shale (Vsh) can also be estimate through SP log, Density and Neutron log. Caliper log evaluates the borehole (BH) geometry and identifies a lithology. Different conditions of logs pattern used for lithology discrimination i.e. straight log pattern shows that clean reservoir formation.

4.4 Porosity

Porosity is defined as the ratio of the volume of voids to the total rock volume, representing the measure of empty spaces within a rock (Donaldson, 2015). It is a crucial parameter in reservoir assessment. High porosity values indicate rocks with a greater capacity to hold fluids. The porosity of rocks varies based on factors such as grain size, sorting, and cementation, typically falling within the range of 5% to 50% in reservoir rocks. Total porosity is determined using Sonic, Density, and Neutron logs, either

individually or in combination. Effective porosity, crucial for reservoir evaluation, is calculated by accounting for the influence of shale (Mavko et al., 2009).

Next, we have to calculate porosity parameters such as:

- Density porosity
- Sonic porosity
- Effective porosity
- Neutron porosity (Given)

4.4.1 Density Porosity

Density-derived porosity is determined by measuring the bulk density of the formation, where the measuring parameter involves a combination of the rock matrix and fluid (George, 1982; Rider, 1995). The combination of Density and Neutron logs is particularly significant for detecting hydrocarbons, with a crossover between them often indicating the presence of hydrocarbons. The calculation of density-derived porosity is performed using the following equation (George, 1982).

$$\Phi_{\text{density}} = \frac{P_{log-} P_{Matrix}}{P_{Fluid-} P_{Matrix}}$$

Where,

P_{log}= density of formation.

P_{Matrix} = density of matrix

P_{Fluid-} = fluid density.

Different matrices densities are as follows:

Sandstone = 2.6 (g/cc)

Fresh mud = 1 (g/cc)

Salt mud = 1.1 (g/cc)

4.4.2 Sonic Porosity

Porosity derived from the sonic log is referred to as Sonic porosity. The sonic log measures the transient time of elastic waves, where the lithology and porosity of the formation contribute to slowness. Sonic porosity logs offer various advantages, including porosity determination, lithology identification, facies recognition, and source rock identification. These logs are valuable for identifying fractures, porosity, lithology, overpressure, and stratigraphic correlation. In compact limestone and sandstone, the sonic log typically exhibits low transient time, while porous sandstone tends to show high values of transient time. Porosity can be calculated from the sonic log using the "Wyllie's Average Time" equation (Asquith and Gibson, 2004).

$$\varphi_{sonic}=\frac{\Delta T_{log}-\Delta T_{matrix}}{\Delta T_{fluid}-\Delta T_{matrix}}$$

ΔT_{log} = Transient time of log in formation.

ΔT_{matrix} =Matrix. transient time

ΔT_{fluid} = Fluid Transient time.

Table 4.1: Different transient time at different matrix is as follow:

Matrix	Transit Time [ΔT log (microsec/ft)]
Sandstone	55
Mud	189
Salt	185

Hydrocarbon affects the interval transit time or delay time of formation increase. This influence should be removed because it affects the values of calculated porosities, thus their effect can be corrected via following equation: φ= φ$sonic$* 0.7(gas) (Rider, 1995).

4.4.3 Effective Porosity

The interconnected pores or spaces within a rock that facilitate fluid flow or permeability in a reservoir are referred to as effective porosity. Effective porosity excludes isolated pores and water absorbed on clay minerals. The effective porosity log can be created by utilizing total porosity logs and volume of shale logs. Effective porosity is typically less than total porosity. It is calculated by subtracting the shale volume from the total volume of the rock and is determined by the following formula:

$$\Phi_{eff} = \Phi_{avg}*(1-v_{sh})$$

Where

Φ_{ave} = Average porosity

v_{sh} = Shale Volume

(Rider, 1995).

4.4.4 Neutron Porosity

Neutron log that is helpful for measuring hydrogen content within formation and determination of the porosity of formation (George, 1982). i.e., Count Rate will be low in high porosity rock and vice versa. Neutron strikes with nuclei of formation then loss of energy occurs. hydrogen atoms of same mass collide with neutrons; then maximum loss of energy occurs. Thus, Gas bearing Sands show low neutron porosity value due to low concentration of hydrogen ions and Shales shows, high neutron porosity values. Moreover, neutron porosity is given in the data and calculated by well log w.r.t depth (Donaldson, 2015).

4.4.5 Total Porosity

Total porosity is the sum of the porosities (average porosity), that are estimated through sonic and density log divided by number of logs. Total porosity is calculated through using the formula:

$$\Phi_{ave} = \sqrt{\frac{\Phi density + \Phi Neutron}{2}}$$

Where,

Φ_{ave} = Total/Average porosity.

$\Phi_{density}$ = Density porosity.

$\Phi_{Neutron}$ = Neutron porosity.

(Rider, 1995).

4.4.6 Saturation of Water

The quantity of pores volume that filled up with formation water is known as water saturation and water saturation can be calculated by having resistivity of water (Rw). Different models that are used for water saturation i.e. Archie's equation, Indonesian and Dual-Water-Based on the lithology. For Clean Sand, Archie's eq. gives an accurate result. Indonesian eq. is used for the calculation of water saturation.

$$Sw = \sqrt{\frac{1}{RT}} \Big/ \left(\frac{Vsh^{(1-0.5*Vsh)}}{\sqrt{Rshl}} + \sqrt{\frac{PHIE^{m}}{a*Rw}} \right)$$

Where

RT=True resistivity of formtion

Vsh= Shale Volume.

Rshl=Resistivity of shale.

PHIE=Effective porosity.

Rw=water resistivity value.

m=Cementation factor.

a=Turosity factor.

Rw is important for water saturation. It can be calculated by having various parameters such as bottom-hole temperature, surface temperature, water salinity in ppm and SP (static. There are two methods that has been utilized for Rw: Pickett Cross plot method and SP method) (Amigun et al., 2012).

4.4.7 Pickett Cross Plot Method:

The resistivity of water can be calculated using one of the simplest and most effective cross-plot methods known as the Pickett Crossplot. This method provides estimates of water saturation and aids in determining formation water resistivity (Rw), cementation factor (m), and matrix parameters for porosity logs. The Pickett Crossplot is based on the observation that true resistivity (Rt) is a function of porosity, water saturation (Sw), and the cementation factor (m). A Pickett Crossplot is developed by plotting porosity values against deep resistivity values on a two-by-three cycle log paper (Pickett, 1972).

The Pickett plot method is employed to calculate the resistivity of water. The X and Y axes of the Pickett plot represent deep resistivity and porosity log, respectively, and it is constructed based on the logarithmic form of Archie's equation. The plot features a straight line with a negative slope representing the volume of m, and the saturation point (Sw) is plotted on this line. The lowest line on the plot defines the zones of water, with (Sw=1) allowing the determination of water resistivity at a specific location on the line. Once the water line is established, additional parallel lines with varying (Sw) values can be drawn, assuming a constant n. Other data points can then be plotted and assessed in relation to Sw. The Pickett plot is utilized to calculate the resistivity of water in both wells.

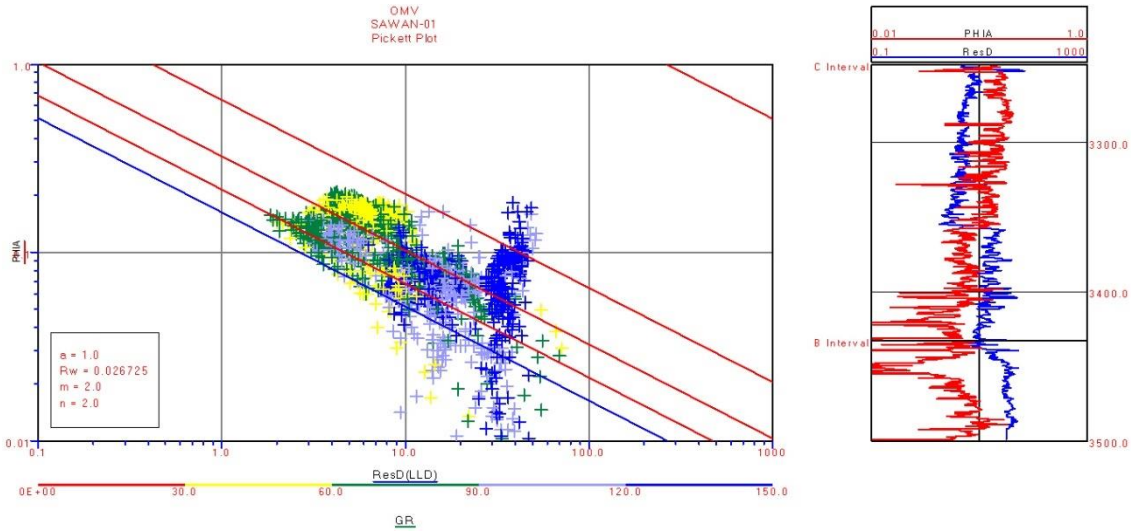

Figure 4.1 Resistivity of water for Sawan 01 by Pickett plot method.

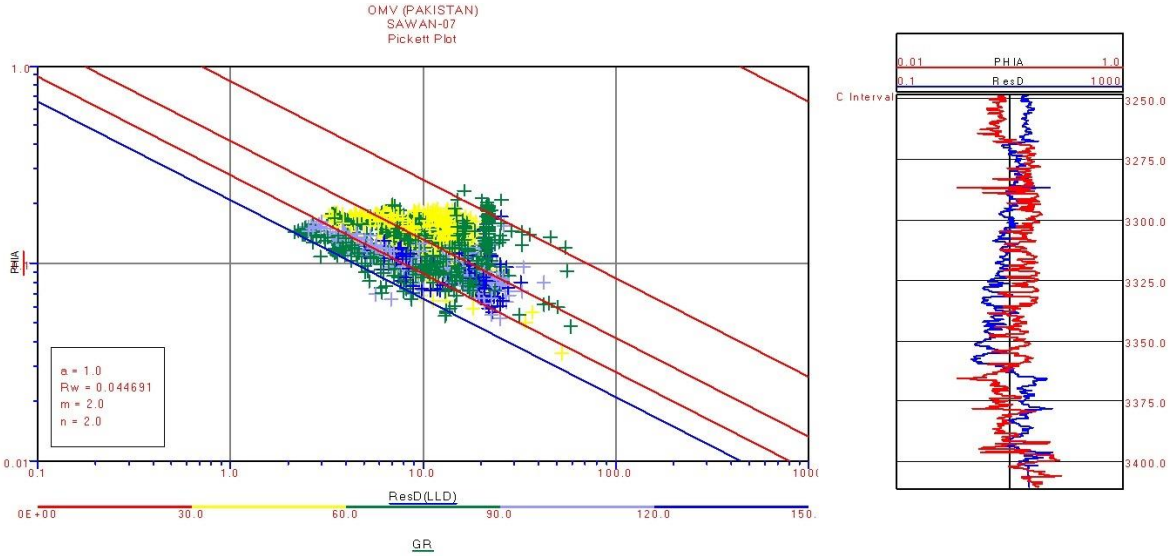

Figure 4.2 Resistivity of water for Sawan 07 by Pickett plot method.

4.4.8 Calculation of Archie Water Saturation (Sw)

The amount of water in a formation is known as water saturation (Ahmed, 2009). Archie's equation provides a mathematical method for calculating water saturation, and resistivity logs are employed for this purpose. The water saturation of the reservoir zone can be calculated using the following formula:

$$S_w = \{(\frac{a*R_w}{R_t*\varphi A})^m\}^{\frac{1}{n}}$$

Where,

- S_w= water saturation,
- φA= average porosity,
- a= lithological coefficient (taken as 1),
- m= cementation factor (taken as 2),
- n= saturation exponent (taken as 2).
- R_t= True Resistivity
- R_w= Water Resistivity

4.4.9 Calculation of Hydrocarbon Saturation (Sh)

Water saturation (Sw) is the percentage of pore spaces that contain water, while hydrocarbon saturation (Sh) represents the remaining fraction containing oil or gas. The formula used to calculate hydrocarbon saturation is given by:

$$Sh = 1 - S_w$$

4.5 Petrophysical Interpretation of B interval

The petrophysical analysis of the B and C intervals of the Lower Goru Formation in the zone of interest was conducted. The process began with loading the LAS files of Sawan 01 and Sawan 07 wells using the Prizm module of the Geographix software. Zones of interest were identified based on the criteria mentioned above. It was observed that, following the specified criteria, two zones were marked in the B interval of Sawan 01 well, and one zone was marked in the B interval of Sawan 07 well. The analysis likely involved assessing the petrophysical properties and characteristics of these marked zones to evaluate their reservoir potential.

4.5.1 Petrophysical Interpretation of B Interval Sawan 01

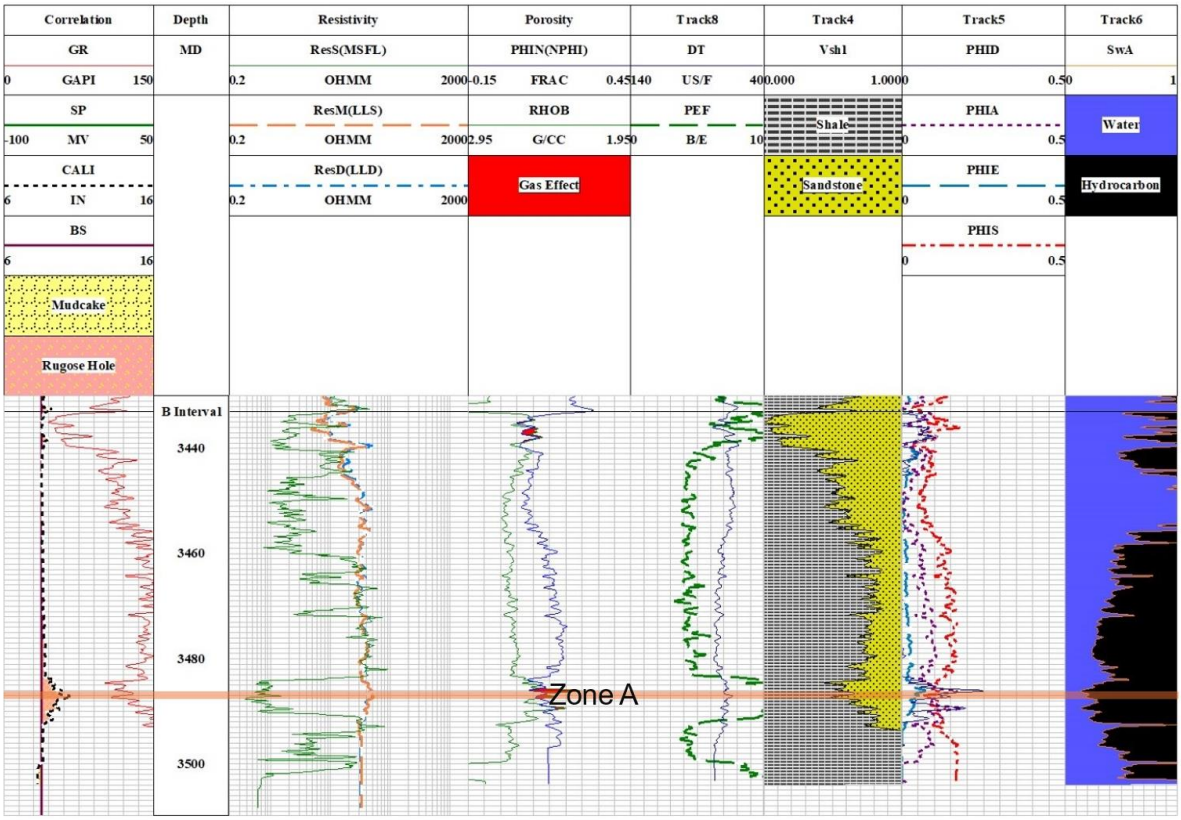

Figure 4.3 Petrophysical analysis of Sawan 01 on B-Interval of Lower Goru Formation.

In the Lower Goru B-Interval of Sawan 07 well, a zone of interest was identified. This zone was observed within the depth range of 3486-3487 m, in the interested zone, the gamma ray value was on the lower side, separation between MSFL and LLD was observed. There was presence of gas effect i.e., neutron and density crossover were observed. And lastly the hydrocarbon saturation was not very good.

In the B Interval of Sawan 01 well, a single zone of interest was identified at depths ranging from 3486 to 3487 meters. leading to the exclusion of criteria related to the separation between MSFL and LLD logs. The identification of this zone of interest in Sawan 01 well was based on the following factors:

1. The presence of a gas effect, likely indicated by a crossover between logs.
2. High values of hydrocarbon saturation within the zone.

It is important to note that within the study area, the presence of radioactive sands can contribute to elevated gamma-ray values. This phenomenon was observed in this specific zone of interest in Sawan 01 well. As a result, the zone was marked as a zone of interest based on the observed gas effect and high hydrocarbon saturation values. Additionally, the impact of shale presence on wireline logging devices was acknowledged, with the gamma-ray device potentially registering large shale volumes due to the presence of radioactive minerals other than shale, such as dolomite and radioactive sands.

4.6 Petrophysical interpretation of C interval

Petrophysical interpretation of the C Interval of Lower Goru Formation in Sawan 01 and Sawan 07 wells involved loading LAS files for both wells using the Prizm module of Geographix software. In the reservoir zones of interest within the C interval of Sawan 01 well, two zones were identified and marked for further analysis. The interpretation likely included assessing various well logs and petrophysical properties within these zones to understand the reservoir characteristics and potential hydrocarbon saturation.

4.6.1 Petrophysical Interpretation of C Interval Sawan 01

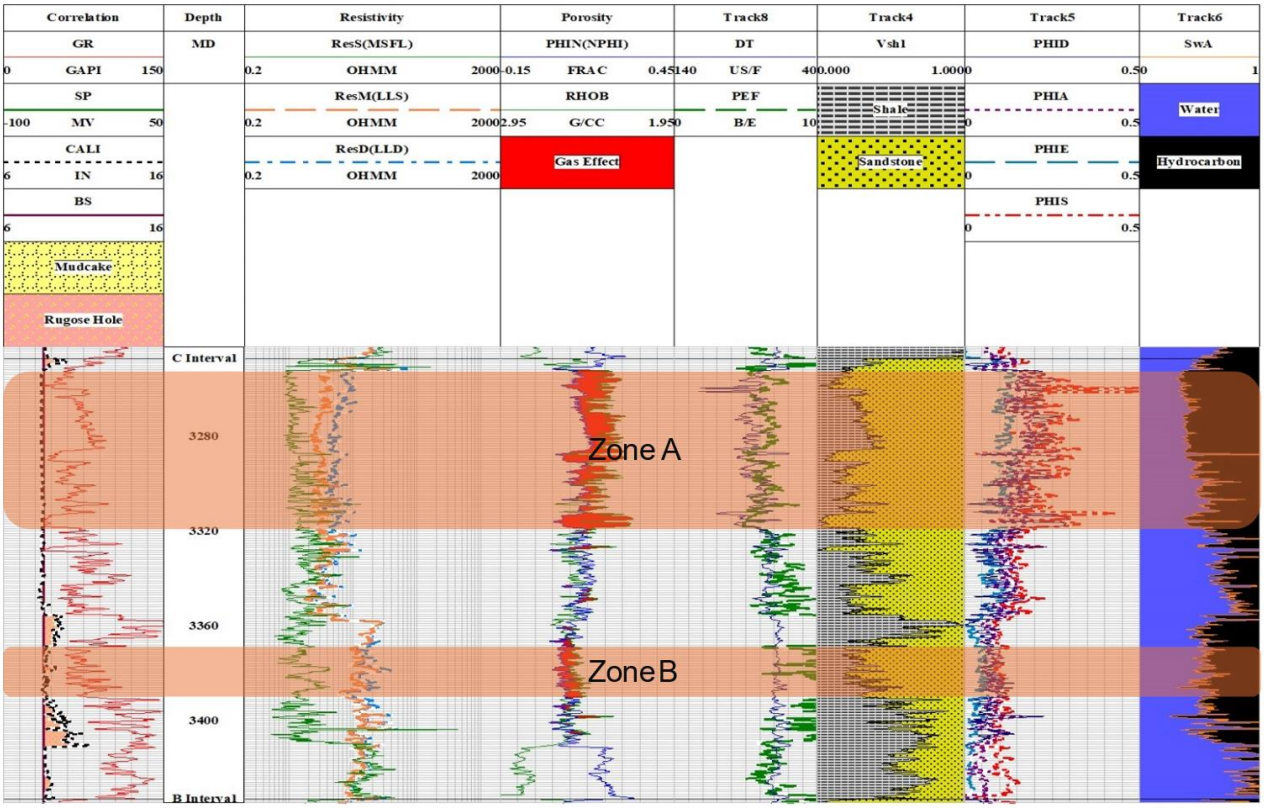

Figure 4.4 Petrophysical analysis of Sawan-1 C-Interval of Lower Goru Formation.

Two zones of interest were marked in the Lower Goru C- Interval of Sawan 01 well. The first zone was observed at the depths of 3268-3387 m, and the second zone was observed at the depth of 3368 to 3387 m.

Within both these zones the gamma ray value was on the lower side, separation between MSFL and LLD was observed. There was presence of gas effect i.e., neutron and density crossover were observed. And lastly the hydrocarbon saturation was also good.

4.6.2 Petrophysical Interpretation of C Interval Sawan 07

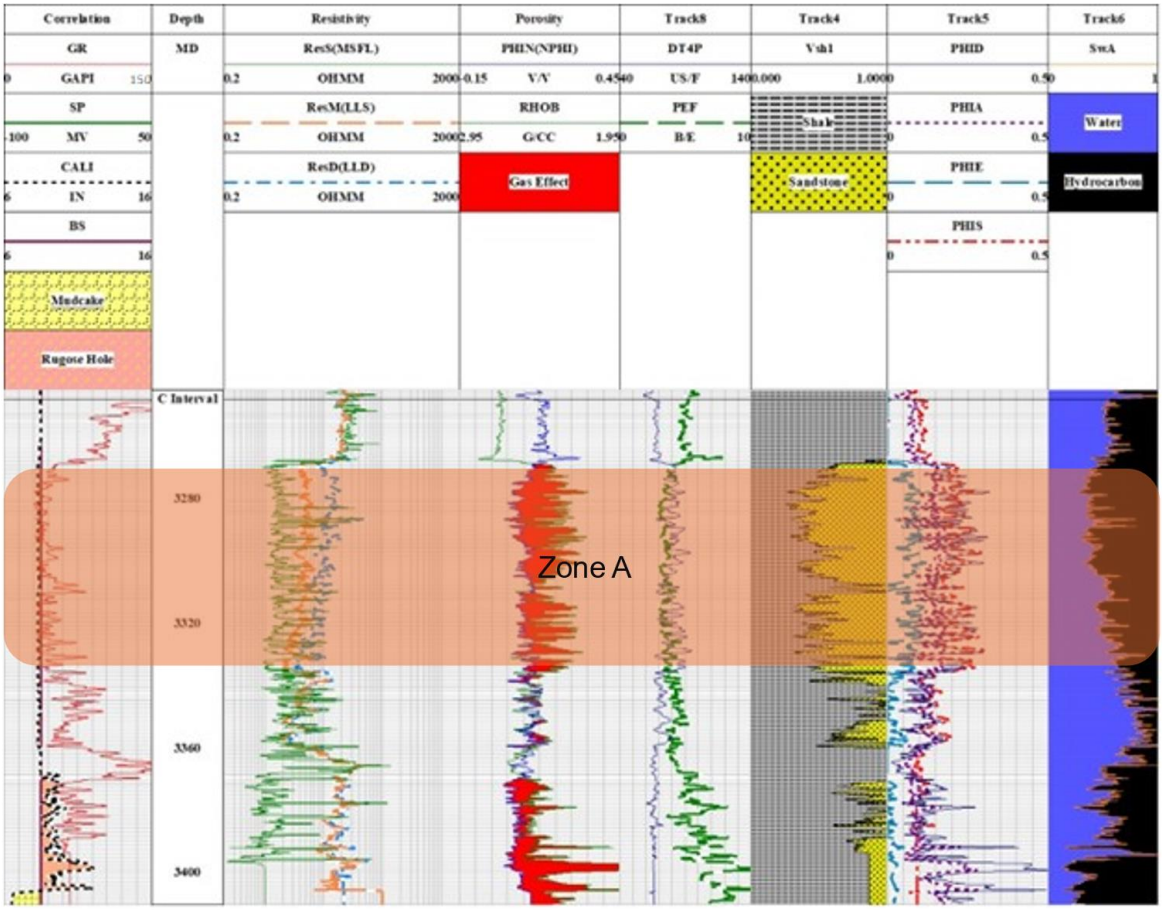

Figure 4.5 Petrophysical analysis of Sawan-7 C-Interval of Lower Goru Formation.

A zone of interest was marked in the Lower Goru C-Interval of Sawan 07 well it was observed at the depth of 3272 to 3335 m.The criteria to mark the zone of interest based on the separation between MSFL and LLD was ruled out. However, within the zone there was presence of gas effect i.e., neutron and density crossover was observed. And lastly the hydrocarbon saturation was also good.

4.7 Results of Petrophysical Interpretation

Table 4.2: Result of petrophysical analysis of reservoir zones

Well Name	Hydrocarbon Zone	Depth(m)	Vshl %	PHIA %	PHIE %	SwA %	Sh %
Sawan 1 C Interval	Zone 1	3268-3387	10	11	7	45	55
	Zone 2	3368 to 3387	11	10	9.1	61	39
Sawan 7 C Interval	Zone 1	3272 to 3335	19	21	17	42	58

CHAPTER NO 5

ROCK PHYSICS AND FLUID REPLACEMENT MODELING

5.1 Introduction

Rock Physics Modeling is the anticipation of variations in P and S waves and the occurrence of Poisson's ratio. It illustrates the absent log prediction, particularly for S-wave, necessitating the establishment or acquisition of elastic properties. This method aids in forecasting anomalous (mostly density logs) or missing S-wave logs while mitigating uncertainties associated with seismic attribute interpretation. Rock Physics Modeling serves as a crucial parameter in establishing connections between elastic properties like impedance and reservoir velocities (Miguel Bosch et al., 2010).

The correlation between rock properties is elucidated in terms of Elastic moduli, which are subsequently utilized for velocity computations (Wawrzyniak-Guz, 2019).

5.2 Fluid replacement modeling

Reservoir rock assessment in AVO primarily employs fluid replacement modeling (Ross, 2000; Russell et al., 2003). Fluid replacement facilitates a deeper comprehension of seismic properties and pore fluids, relying on various saturations such as water, gas, and oil (Gassmann’s relation, 1951).

5.3 Workflow of Rock Physics

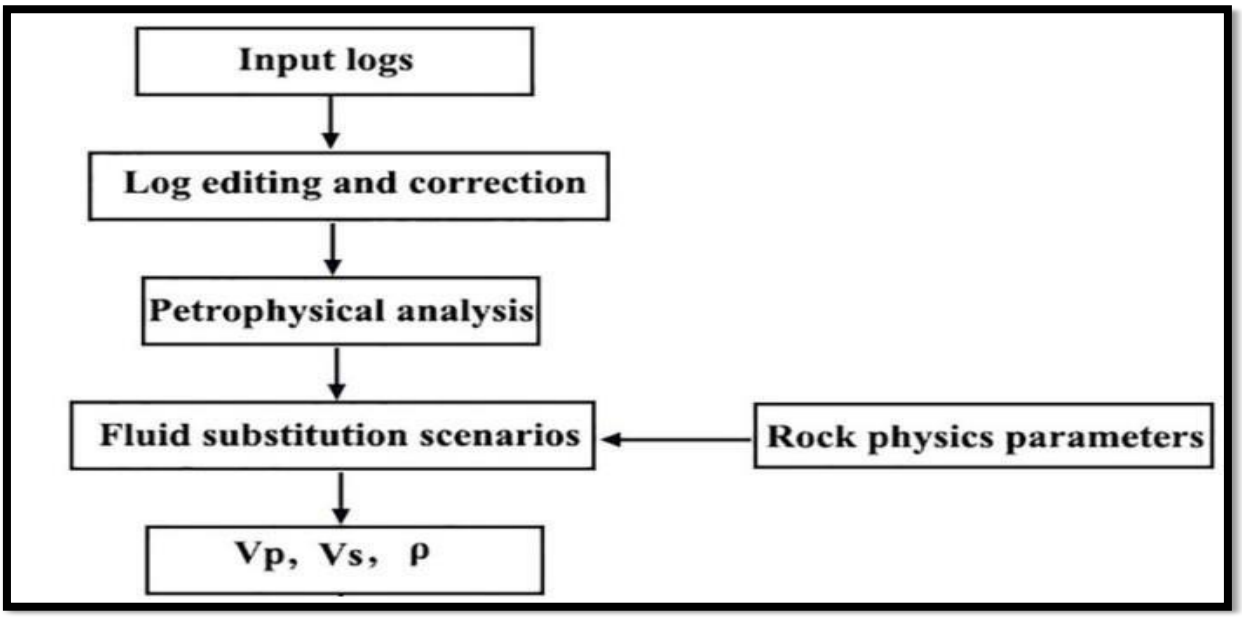

Figure 5.1 Fluid replacement workflow

5.4 Scenarios in for fluid substitution

Different types of fluids, including water and gas, were introduced and substituted into reservoirs in varying proportions. This approach aimed to evaluate and better assess the quantitative parameters of the appropriate fluids present in the reservoir by depicting amplitude matching. Three primary scenarios were considered:

- Insitu case (80% gas 20% water)
- Gas 100 % and water 0 %
- Gas 50% , water 50%

5.4.1 Insitu case (80% gas 20% water)

Insitu case we exert 80 % gas and 20% water as substitution method to see the results ofthe curves how it responds and their variations of behavior.

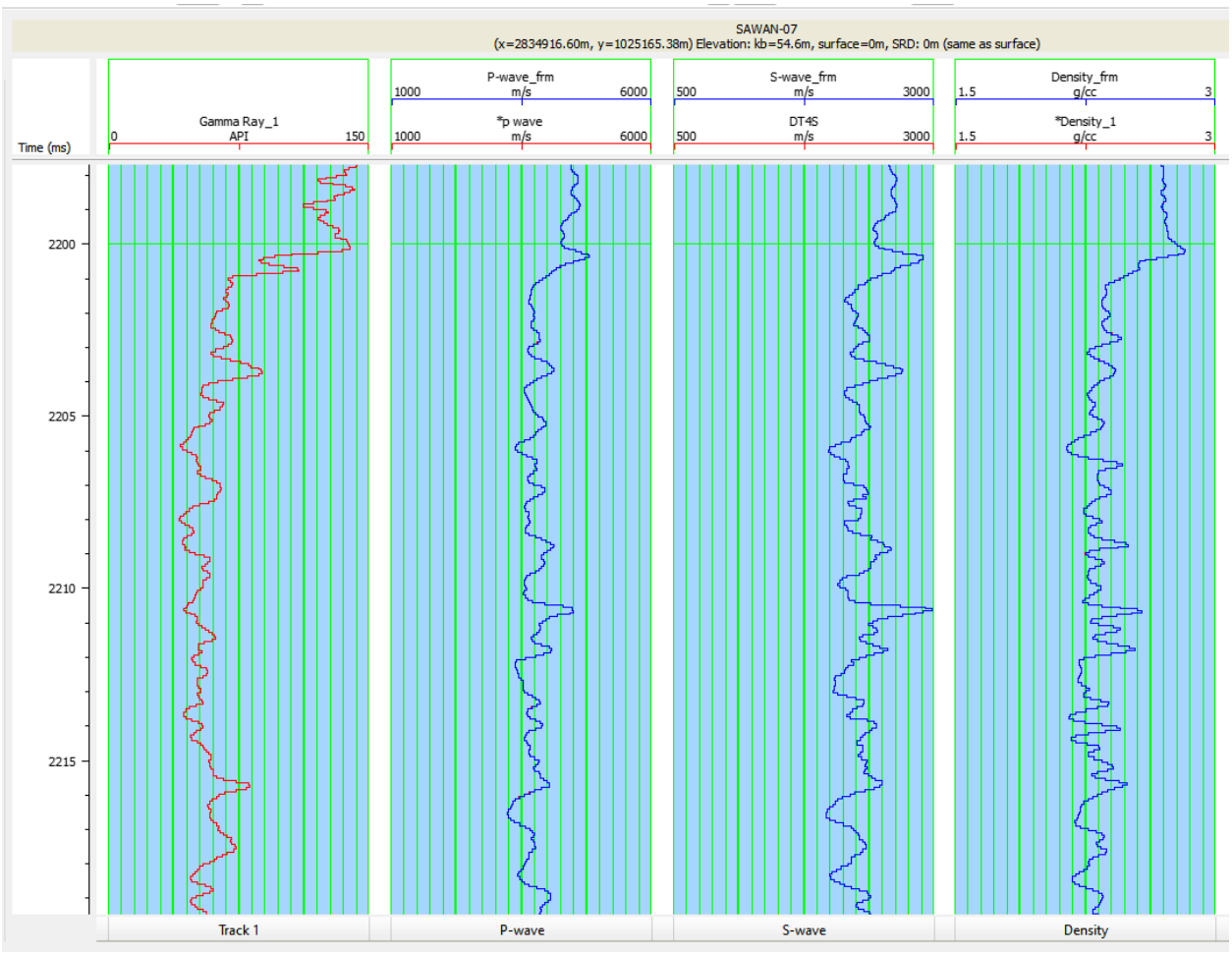

Figure 5.2 Depicts that Insitu condition holds substitution of 80% Gas and 20% water scenario.

5.4.2 Gas 100 % and water 0 %

In Second case we exerted 100 % gas and 0% water as substitution method to see theresults of the curves how it responds and their variations of behavior.

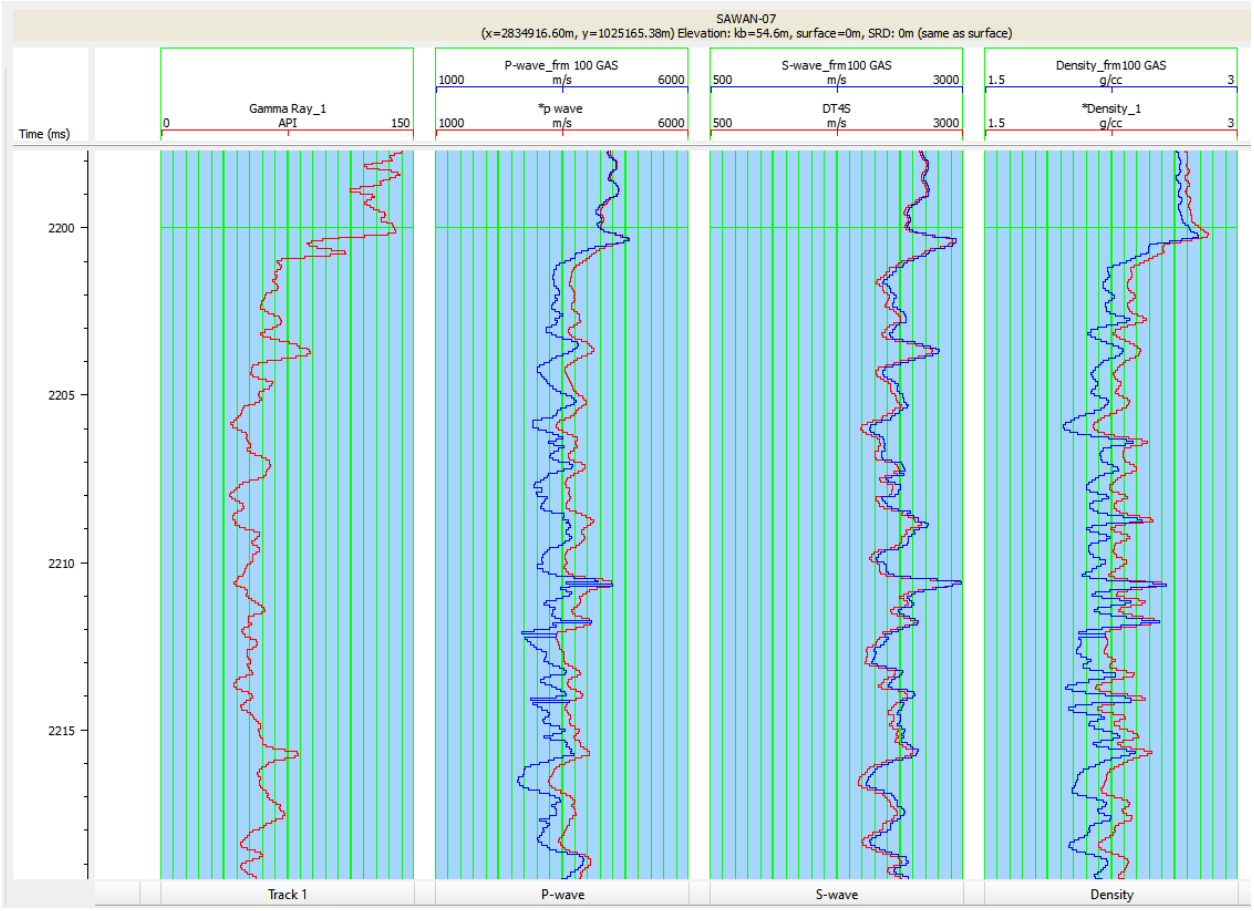

Figure 5.3 Depicts that substitution of 100% Gas and 0% water scenario.

5.4.3 50% gas 50% water case

In Third case we exerted 50 % gas and 50% water as substitution method to see theresults of the curves how it responds and their variations of behavior.

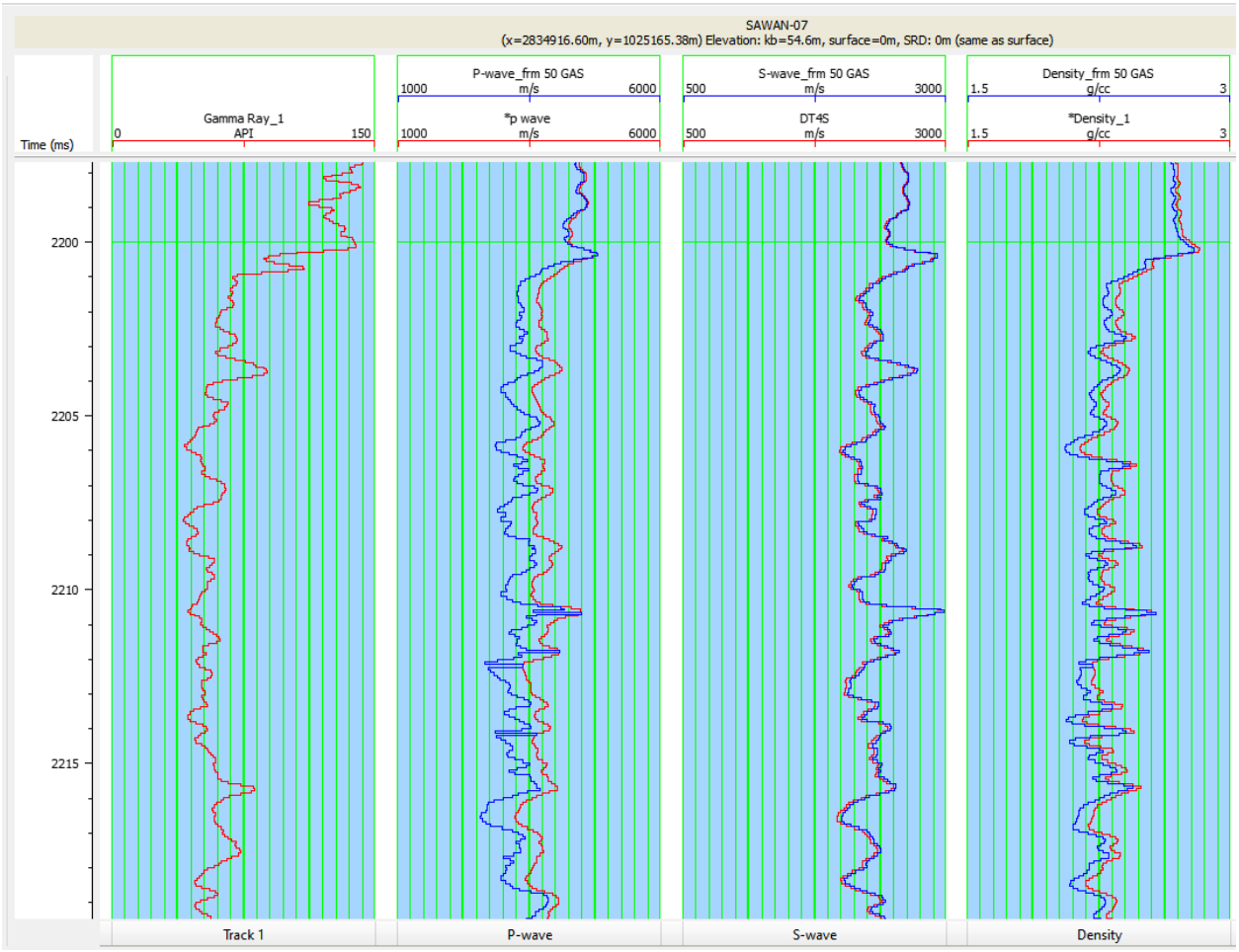

Figure 5.4 Depicts that substitution of 50% Gas and 50% water scenario.

5.4.4 Outcome

As shown in the figure we have substituted different scenarios and exerted values and made S-Wave Prediction. Lower Goru C Sand interval is acting reservoir and have lot of potential to act as reservoir.

CHAPTER NO 6

SEISMIC INVERSION TECHNIQUE FOR RESERVOIR CHARACTERIZATION

6.1 Introduction

Seismic inversion, which is a subsurface geological modelling approach uses well-data as a control and seismic data as an input. The seismic inversion is carried out by converting the data in amplitude form to the impedance form (Kianoush et al., 2023). Seismic inversion enhances interpretation by helping to identify the significant subsurface geological and petrophysical boundaries (Talib et al., 2022). Seismic inversion is one of the known methods for extracting valuable information from seismic data, interest in it has been growing steadily over the past few years. Seismic inversion also enhances the resolution of conventional seismic. Deterministic and probabilistic are the methods of inversion and the approaches are either pre or past stack (Veeken and Silva, 2004).

The procedure of turning seismic reflection data into seismic impedance is called seismic inversion. Acoustic impedance is a layer property since it is related to the layers rather than interface and it is the product of density and velocity (Onajite, 2014).

As acoustic impedance changes with lithology, porosity, fluid content, pressure, depth, temperature etc. Thus, it can be used as an indicator of lithology to precisely map flow unit, an indicator of porosity, an indicator of hydrocarbons and a tool for quantitative analysis. Thus, the result of inversion has a substantial impact on interpretation and ultimately decision making in the industry (Jain, 2013).

Earth's properties are reconstructed by seismic inversion, and it is readily employed in the industries of oil and gas. For the prediction of porosity and lithology it combines well data and seismic data. These characteristics of rock may be applied for the identification of hydrocarbons and reservoirs (Kianoush et al., 2023).

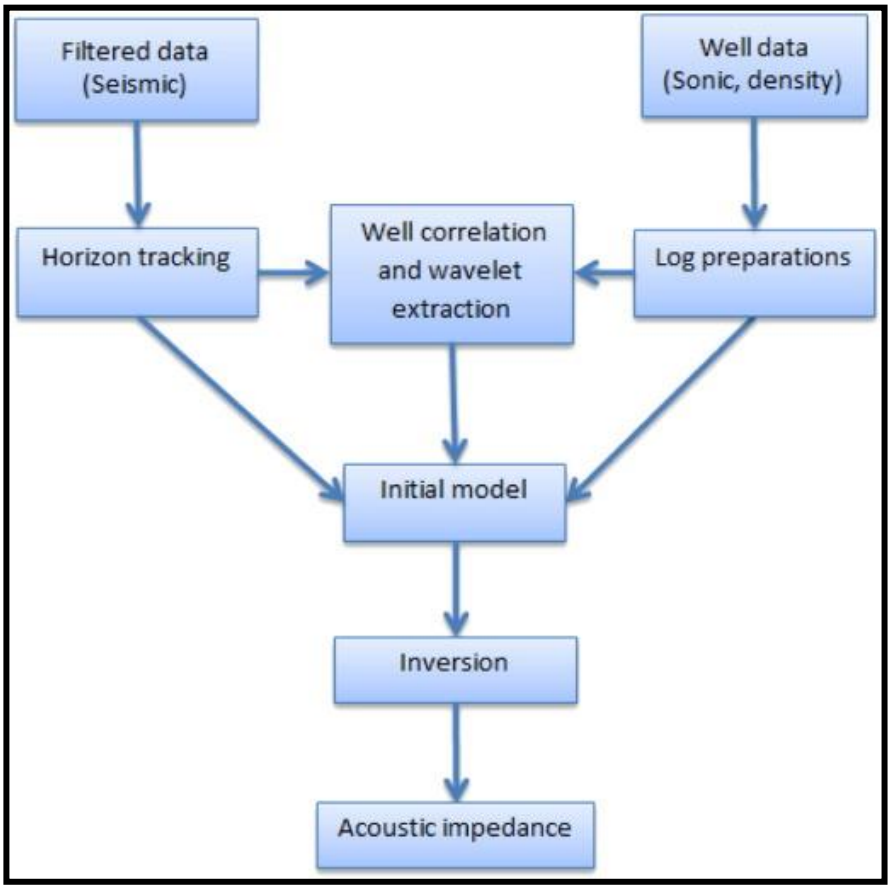

Figure 6.1 Generalized workflow of seismic inversion (Veeken and Silva, 2004).

Pre-stack seismic data and post-stack seismic data are the two types of seismic data that the seismic inversion method deals with. Both pre-stack seismic and post-stack seismic data are used in seismic inversion methods (Kumar et al., 2016). Post-stack seismic data only produces P impedance, whereas pre-stack seismic data also generates P and S acoustic impedance as well as their derivatives, such as Vp/Vs, Lambda-rho, and Mu-rho, which can

be used to estimate fluid and lithology parameters from the subsurface (Barclay, 2008). However, post stack inversion is performed in this research.

6.1.1 Seismic inversion's purpose

The main objective of seismic inversion is to convert seismic reflection data into quantitative rocks properties that describe the reservoir. Acoustic impedance logs are calculated at each CMP in their most basic form (Barclay, 2008). Results using inversion improve resolution and support more precise interpretation as compared to working with seismic amplitude. This then makes it easier to estimate the reservoir characteristics like porosity and net pay (Pendrel, 2001).

Other advantages of seismic inversion include:

- Wavelets impacts within the seismic bandwidth are eliminated by using seismic inversion (Kianoush et al., 2023).
- Overburden is separated from reservoir properties.
- Impedance domains interpretation is typically simpler than seismic domain interpretation (Kianoush et al., 2023).

6.2 Post Stack Inversion

Post stack inversion procedures as the name implies pertain to a variety of methods used for transforming the stacked seismic data into quantifiable rock physics parameters. Porosity, saturation, shale content, and other reservoir properties are estimated using post-stack seismic inversion (Abosalama, 2022).

Acoustic impedance is often the product of post stack inversion’s product is the Acoustic Impedance however, both acoustic and shear impedance can be produced by pre stack inversion. With its simple assumptions seismic post-stack inversion is a reliable approach. It uses two distinct approaches: band-limited and broad band inversion (Karim et al., 2016).

6.3 Model Based Inversion

In the geophysical community, model-based seismic inversion is very common because it provides quick and accurate estimations of acoustic impedance. In a model-based inversion, the wavelet is convolved with the simplistic initial acoustic impedance model to produce a synthetic response that is compared to the actual seismic trace (Kianoush et al., 2023).

To create a synthetic seismic trace, using this method, the seismic trace (initial model) is convolved with a wavelet. Next, until the difference between the initial trace and invented trace is decreased to a limit value, the image is subjected to numerous iterations (Russell, 1988).

The output is free of noise component that is nearly always present with the seismic data because the model-based inversion does not use raw seismic data. Since the seismic data is band limited and direct inversion methods cannot provide the precision and accuracy needed by the exploration sector, model-based inversion is effective for thin reservoirs (Russell, 1988). High frequency and low frequency components both are present in the model based seismic inversion thus providing detailed information on stereographic and physical properties (Russell, 1988).

$$J = weight\ a \text{ x } (S - W * R) + weight\ b \text{ x } (M - H * R)$$

The seismic trace is denoted by S in the equation, the wavelet recovered from seismic data is donated by W, the reflectivity series is denoted R, the initial model is donated by M and H is integration operator (Russell, 1988).

Given the initial half of the equation is obviously modelled with seismic trace while the other part is modelled using an estimated initial model. Seismic trace was modeled in the first quarter of equation and the estimated impedance was modelled in the second portion (Russell, 1988).

6.4 Methodology adopted for Model Based Inversion

The model-based algorithm of post stack inversion is performed by using Hampson and Russell software. The methodology utilized for conducting the model-based seismic inversion is outlined in the workflow provided below (Figure 6.2).

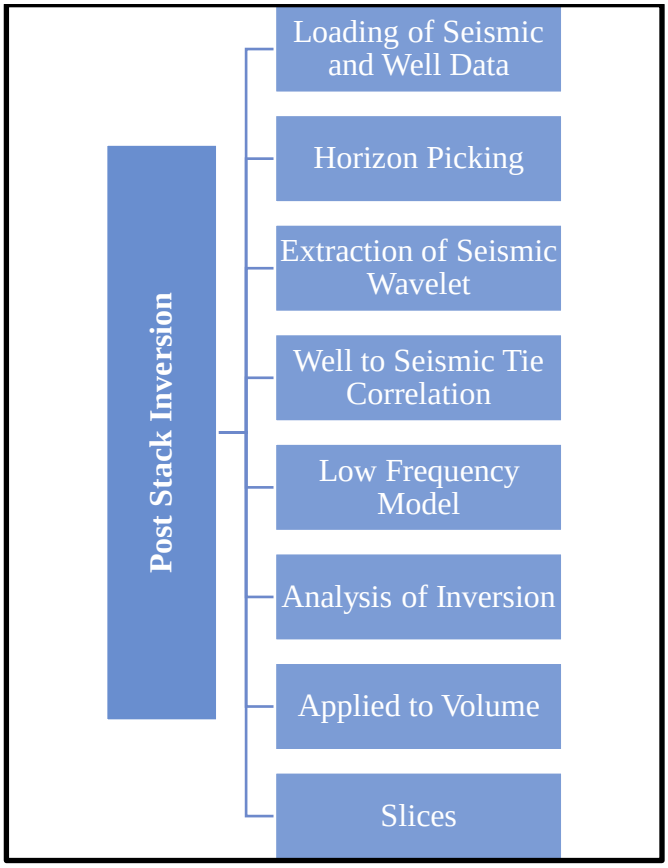

Figure 6.2 Workflow Adopted for Modal Based Inversion

6.4.1 Seismic and Well Data Loading

The loading of seismic and well data into Hampson and Russell software is the first step in post-stack inversion. The 3D cube of Sawn Gas Field is loaded into the software along with interpreted well data in Las format, following data loading the location of well is matched with seismic data for confirming the exact location of well in the seismic cube.

6.4.2 Loading of Horizons

The next step involves loading of horizons in the seismic section. The interpreted horizons are exported in time amplitude format from Kingdom Software. After that these horizons are imported in HRS software. The horizons of B and C intervals of Lower Goru Formation were imported.

6.4.3 Extraction of statistical wavelet

One of the most important steps in quantitative interpretation is wavelet estimation. The outcomes of seismic inversion depend on the quality of the wavelet, which in turn determines the quality of the seismic correlation. The seismic wavelet is an essential link between seismic data and subsurface stratigraphy and rock characteristics (Cui et al., 2014).

6.4.4 Seismic to Well Correlation

This study employs the sonic (compressional wave velocity) and density logging information from the Sawan-07 well to estimate the acoustic impedance of the subsurface strata. This is then aligned with the seismic data from In-line 791 for a comparative analysis as illustrated in Figure 6.6. The first column of the figure presents the compressional wave velocity profile along the entire depth of the well, whereas the third column displays the density measurements for the Lower Goru formation's reservoir section. The synthetic trace, depicted in blue in the fourth column, is created using a Ricker wavelet as the base wavelet. In contrast, the red trace in the same column represents the actual seismic data collected from In-line 791. By comparing the synthetic and real seismic traces, the intervals B and C within the Lower Goru formation are identified on the seismic section of In-line 791.

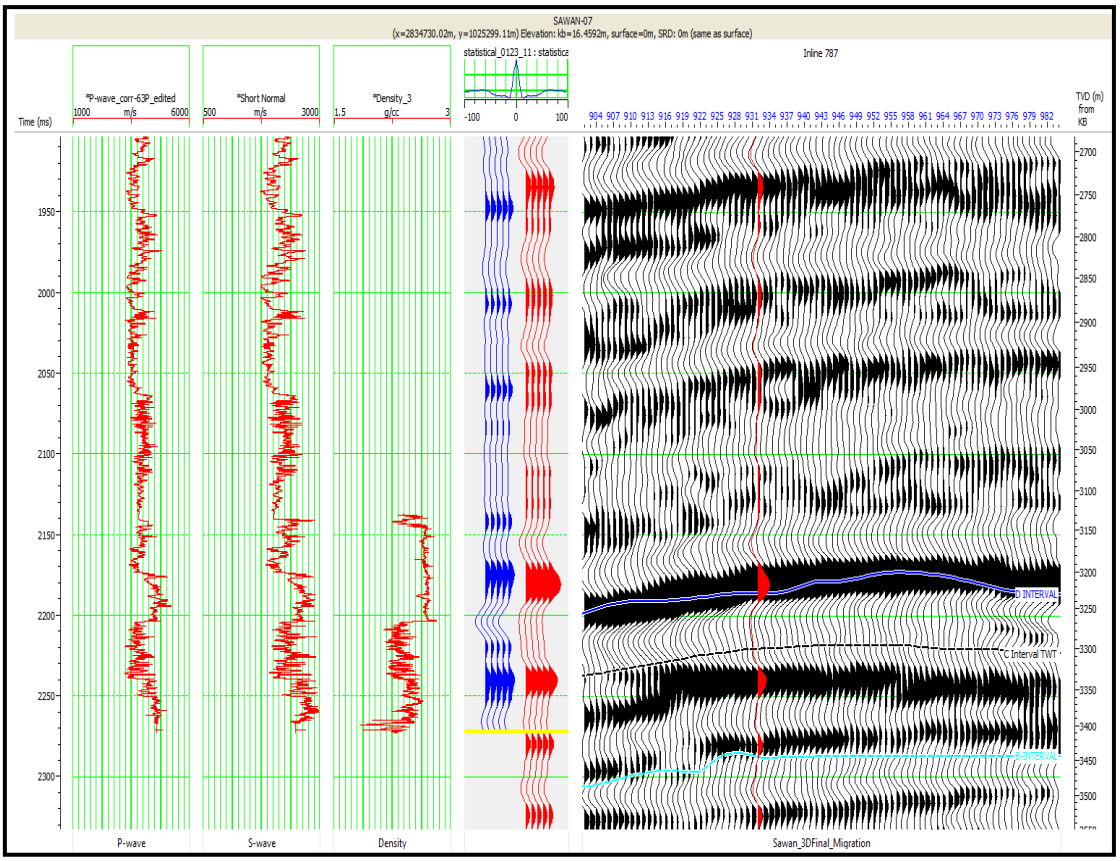

Figure 6.3 Correlation of seismic data with Sawan-07 well.

6.4.5 Initial Low Frequency Model

The initial low frequency model is estimated using acoustic impedance. The acoustic impedance is divided into 2 types namely relative and absolute acoustic impedance (Sams and Carter, 2017). It is not necessary to create a low frequency model to calculate the relative acoustic impedance. Because of the relative qualities of the strata, it is favorable for qualitative interpretation of seismic sections (Li et at., 2013). Integration of low frequency model during seismic inversion improves the qualitative and quantitative interpretations levels of seismic inversion results. Well data Information is required to build low frequency model. The qualitative and quantitative interpretation gets enhanced by integrating low frequency model during the seismic inversion (Kumar et al., 2016).

Increased resolution, conversion from an interface to a layer property, conversion to physical rock properties (impedances), removal of the wavelet, and reduced tuning are some

of the well-known advantages of seismic inversion. All of these improve the seismic data's interpretability both quantitatively and qualitatively (Latimer et al., 2000).

The production of the absolute impedances requires the integration of an accurate low frequency model with band limited seismic data. For each property for which inversion is to be performed, low frequency models must be built (Sams and Carter, 2017). The properties vary depending on the inverted seismic data, but they are frequently some types of elastic property or a combination of elastic properties (Sams and Carter, 2017).

To aid in the construction of low-frequency models, the following key sources of low frequency data can be used: seismic velocity data and well-log data. There may be measurements for all the necessary elastic characteristics in well log data, which cover the entire frequency range from zero to well above the highest seismic frequencies (P-sonic, S-sonic, and density). A low frequency model is typically created by simply interpolating well data within a structural and stratigraphic framework. The Initial low frequency model must be added to the Model-based Inversion process (Sams and Carter, 2017).

By using density and sonic log in the vicinity of the well, the initial low frequency model is generated. The estimated initial model of low frequency with Sawan-07 is displayed in Figure 6.4. The color scale on the right side of the image corresponds to values of acoustic impedance, which is a measure that combines rock density and the velocity of seismic waves through the Earth's subsurface. Acoustic impedance varies with geological formations and can give insights into the presence of different rock types and potential fluid contents such as hydrocarbons.

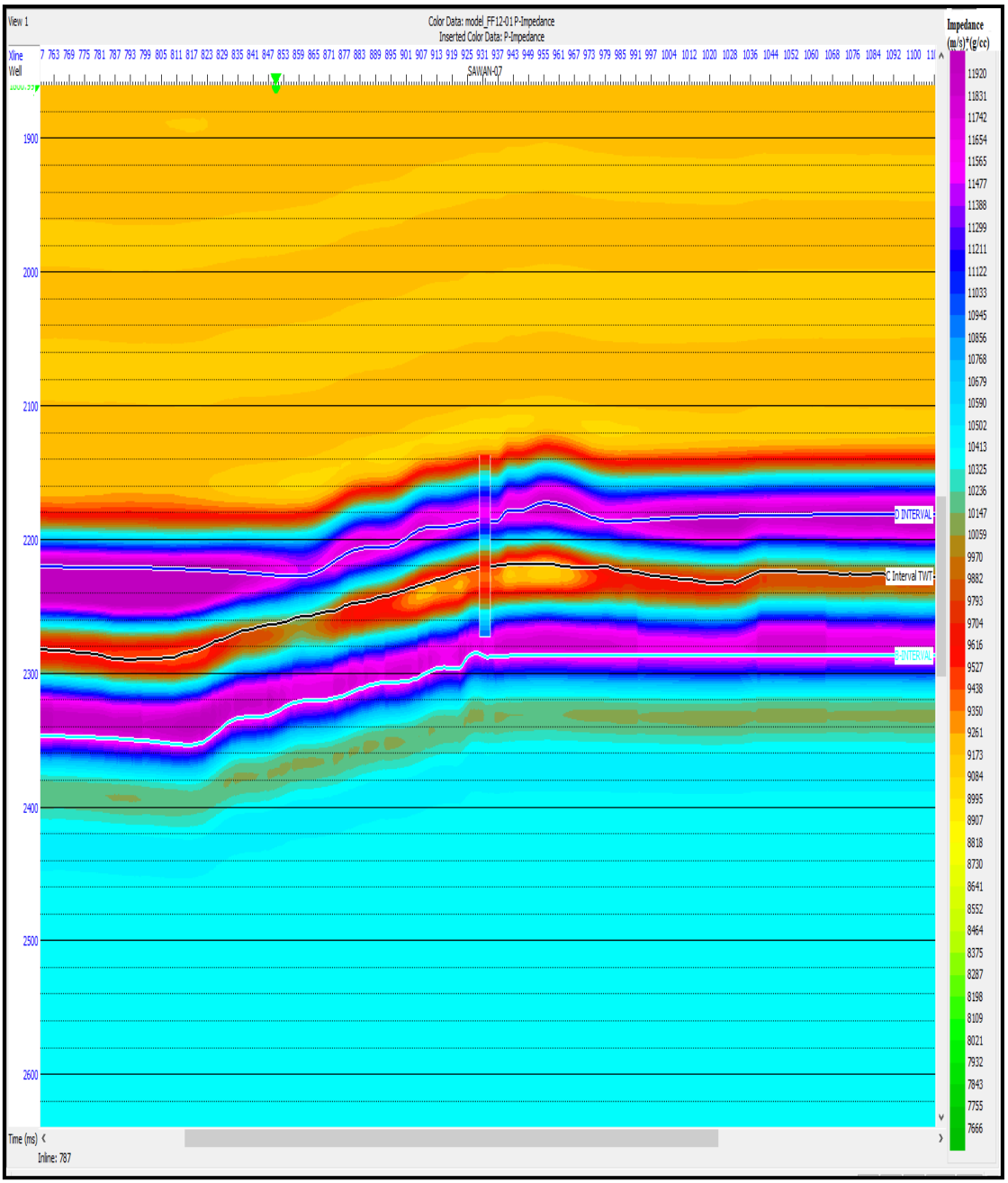

Figure 6.4 Low Frequency model with well location of Sawan-07

The low frequency model of lower Goru formation shows in figure 6.4. In this model all three intervals B and C are marked and displayed with different acoustic impedance contrast. B interval which is purple according to scale bar having higher impedance value ranging from 11388 to 11920 g/cm3-m/s, and C-Interval is showing low impedance values ranging from 8641 to 10059 g/cm3-m/s, which is the indication of hydrocarbon bearing zone.

Well, Sawan-07 is placed over this model for correlation which is showing an exact match of impedance over time section of target zone.

6.4.6 Inversion Analysis

At the Sawan-07 well site, the given seismic cube information was analyzed for model base inversion. The wavelet that was extracted from the time window was between 2200 to 2600 ms. The wavelet that was extracted seismically was adjusted by comparing the synthetic trace with the inverted trace at the well location. A good impedance model will be generated as a result of high correlation percentage. As seen in Figure 6.5 the black color represents the traces and synthetic traces are shown by red color. Sawan-07 is having correlation coefficient of 99.76% with root mean square error between the seismic trace and synthetic is 0.2%.

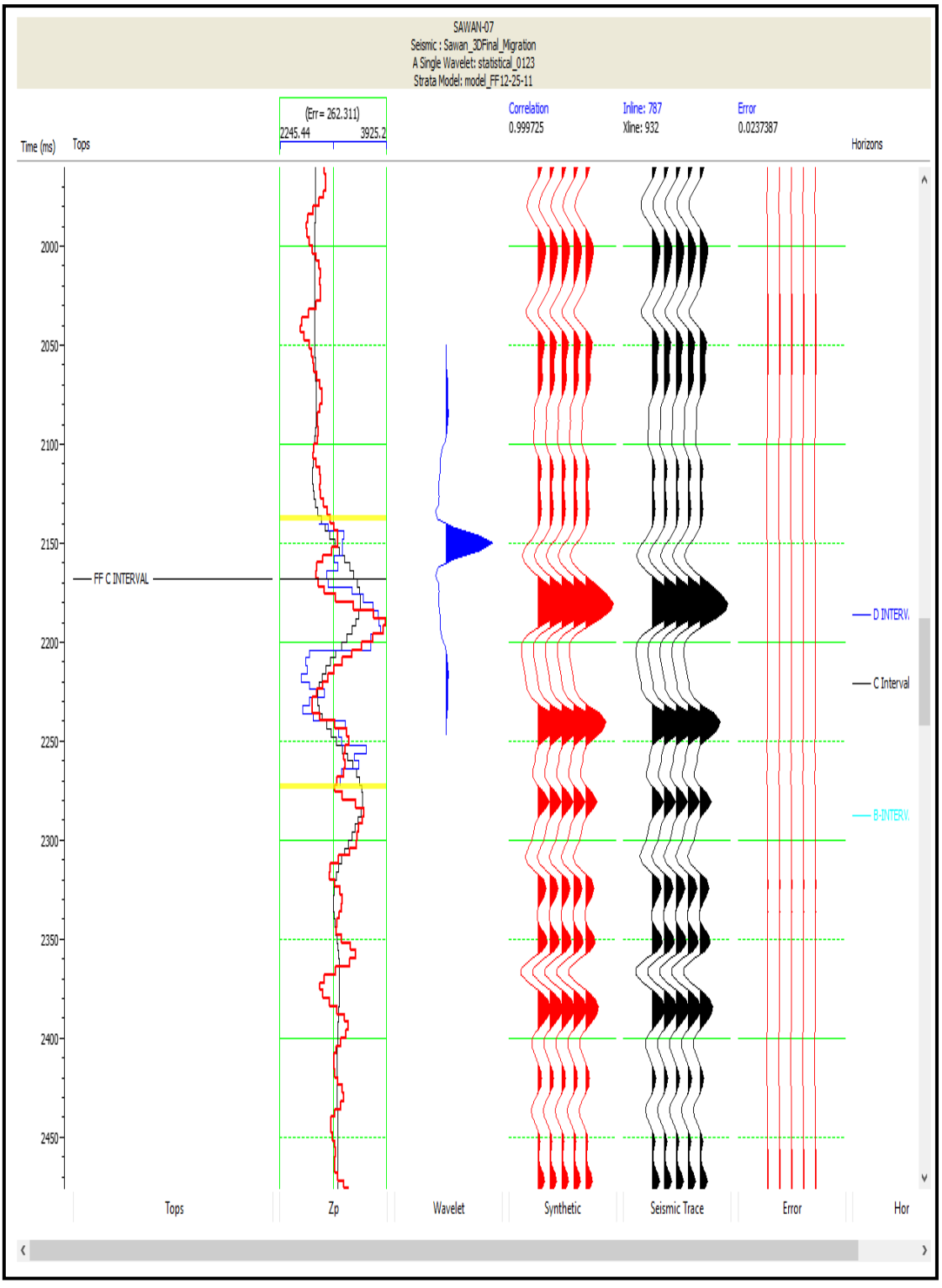

Figure 6.5 Model based inversion analysis of Sawan-07

6.4.7 Results of Model Based Inversion

Physical properties of rock and fluids from seismic data are extracted by seismic inversion (Krebs et al., 2009). The mapping, interpretation, and quantification of hydrocarbon bearing zones have become less challenging by using seismic post stack inversion (Ali et al., 2018). The post stack inversion with zero offset converts seismic data(amplitude) into volume of acoustic impedance contrast by using geological data, seismic, well logs etc. (Downton et al., 2005).

Model-based inversion produces an acoustic impedance model that matches the entire frequency range of impedance by taking low frequency model and seismic data as inputs. The model-based inversion is more realistic and accurate, but an accurate initial model and computation is required for model-based inversion (Narayan et al., 2023).

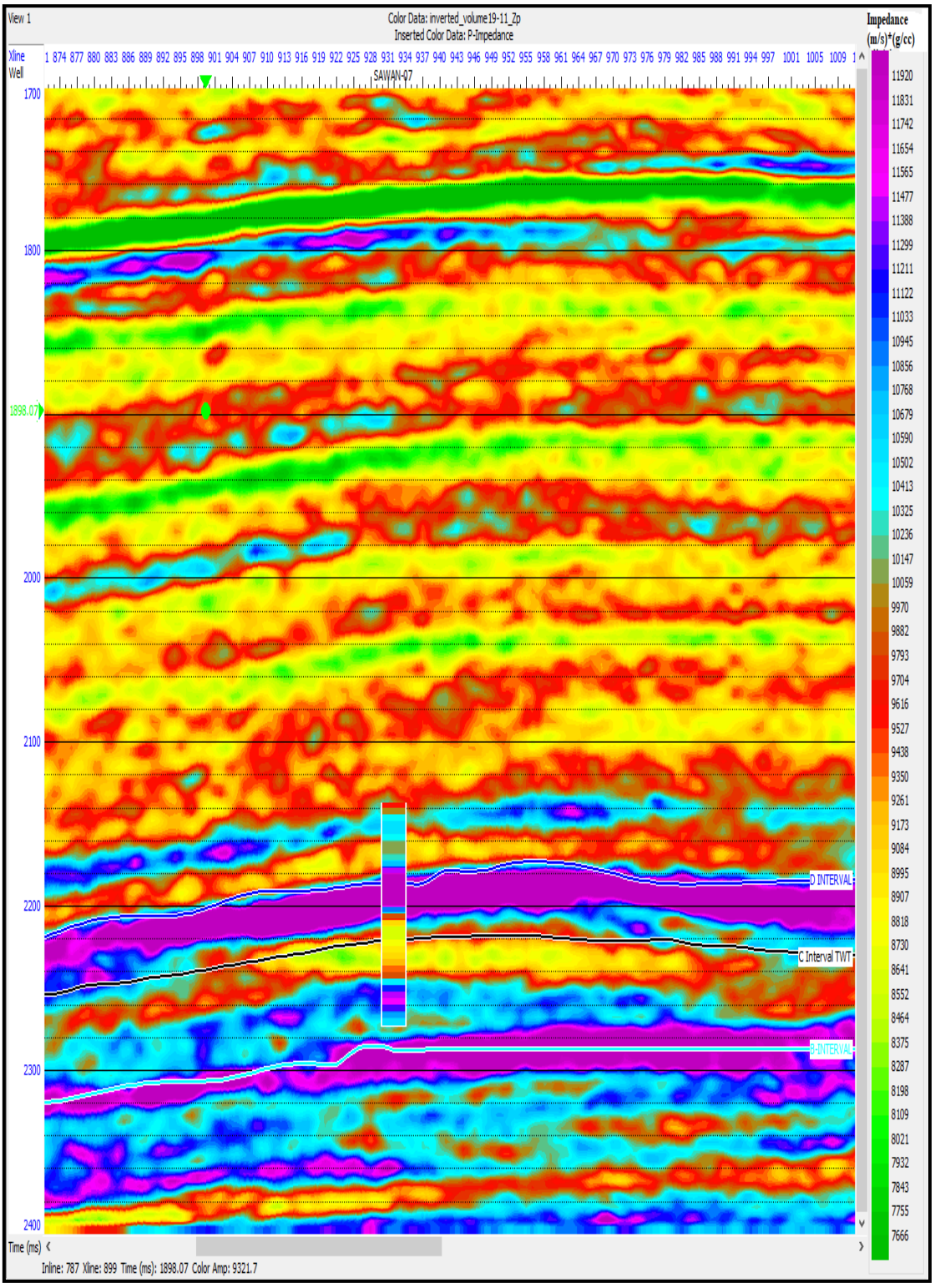

Figure 6.6 Final Computed impedance model at Sawan-07 Well location.

As can be seen in Figure 6.6 the impedance range lies between 7666 to 11920 g/cm^3-m/s. And the C interval of Lower Goru Formation is marked by the impedance of

approximately and 12687 g/cm^3-m/s respectively. Considerably lower impedance values are encountered along the horizons. The low impedance indicates the reservoir zones and might be having gas saturation.

The inverted impedances of well and seismic sections are exact match shows in figure 6.9. the well impedance is placed on time section for confirmation.

6.4.8 Slice of C interval

A 3D slice was generated for the C interval within the Lower Goru Formation (Figure 6.7). This slice displays the overall variation in P impedance across the C interval. Impedance values within the C interval range from 5273.28 to 13102.55 g/cm3-m/s.

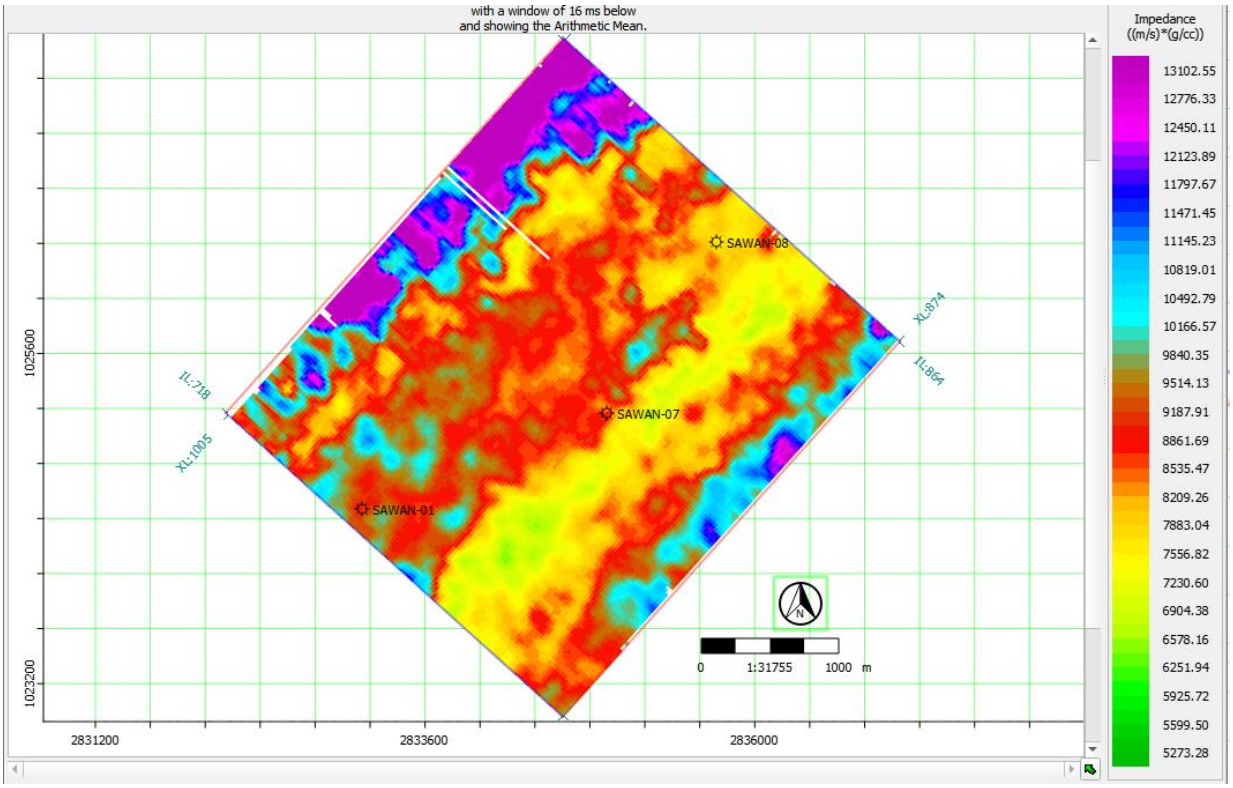

Figure 6.7 3D cube slice for C Interval showing variation for P-Impedance.

Notably, along the Sand channel (C sand), there is a significant anomaly of lower impedance observed at the Sawan-01 and Sawan-07 locations, suggesting a possible accumulation of hydrocarbons (gas). This observation is depicted in Figure 6.7, where relatively higher impedance values are noted in the northern-western and some eastern areas,

while lower values are observed centrally and at the locations of Sawan-01 and Sawan-07. These lower impedance values are indicative of potential hydrocarbon accumulation.

CHAPTER NO 7

MACHINE LEARNING IMPLEMENTATION FOR RESERVOIR CHARACTERIZATION

7.1 Introduction

Machine learning has played a momentous role in the hydrocarbon industry in the last couple of years. Machine learning algorithms will have outstanding results to depict the reservoir characterization by doing firstly Exploratory Data Analysis (EDA) and then comes towards machine learning.

The main Problem starts from Data acquisition problems then Seismic processing like noise removal etc. So, during such setups important data is missed in which we do seismic interpretation and petrophysical analysis. So, to enhance the results we will apply a machine learning approach towards it.

7.2 Methodology

By using Probabilistic Neural Network (PNN) we have calculated Volume of Clay, Porosity and Saturation.

7.2.1 Probabilistic Neural Network (PNN)

PNN is widely used for several years in geophysical studies. It depicits the distance of weighted substance approach to the tiny points for the interpolation (Mahmood et al., 2017).

7.2.2 Volume of Clay prediction using PNN (Machine learning)

Clay plays a vital role in hydrocarbon industry as its minerals plays momentous role in the composition in source rocks as well as reservoir rocks which ultimately is produces and store hydrocarbons. Clay minerals affect the physiology and chemistry of sandstone, limestone's andunconventional shale. We have predicted volume of clay by using PNN.

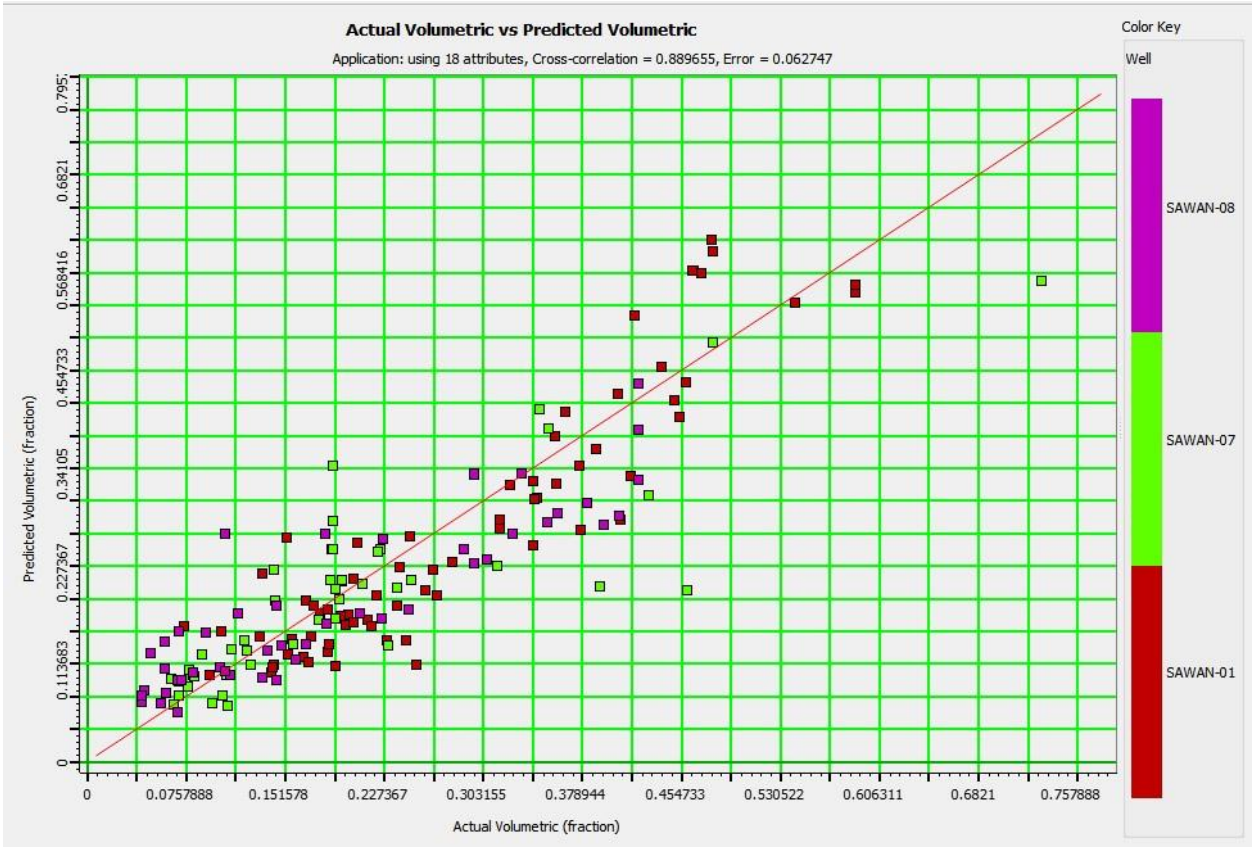

Figure 7.1 Cross plot of Actual Volume of Clay and Predicted Volumetric analysis of Clay (modeled).

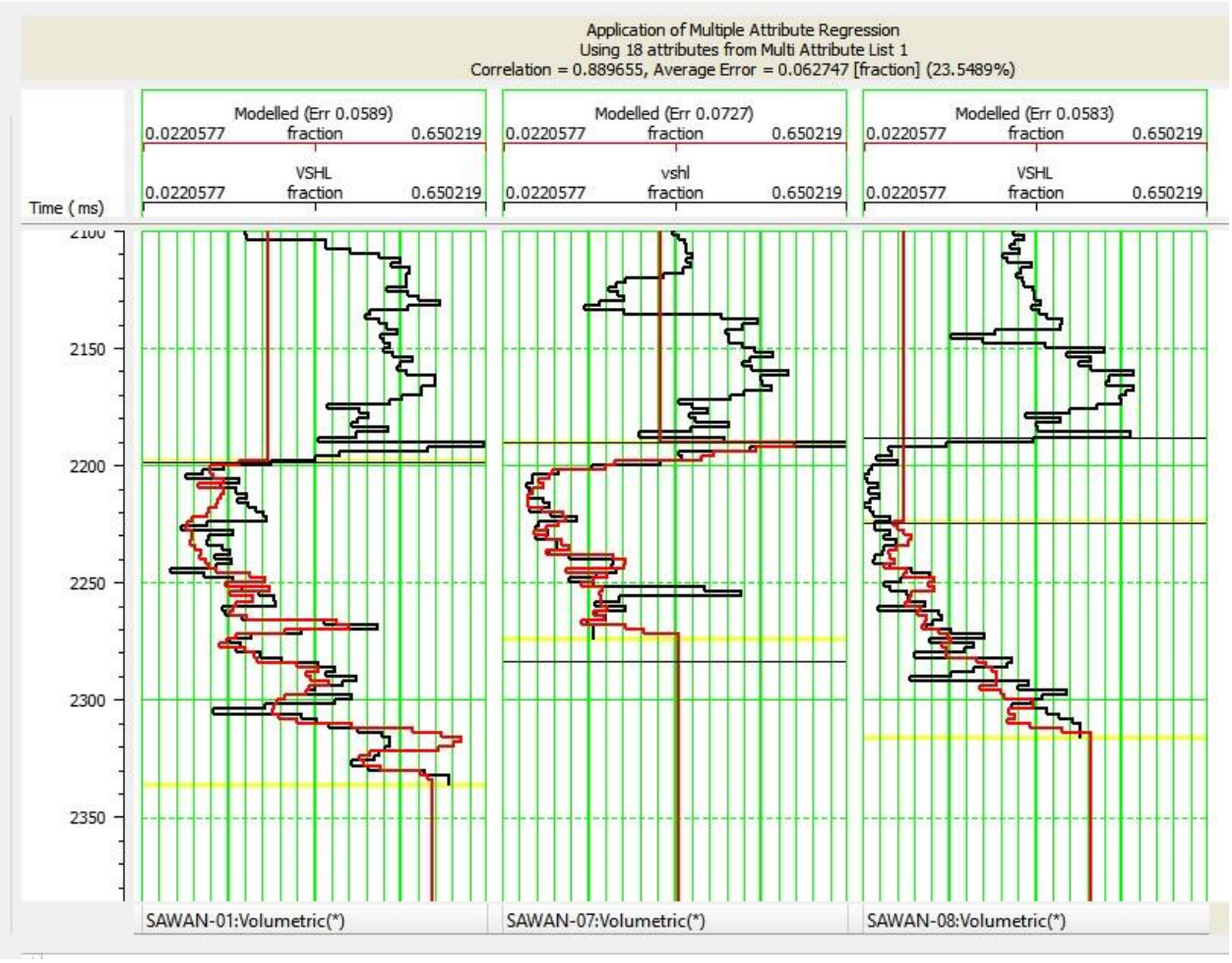

Figure 7.2 Training result of PNN of Actual Volume of Clay and Predicted Volumetric analysis of Clay(modeled).

7.3 Results

The correlation between Actual (Black, Petrophysically calculated) and Predicted (Red,PNN) volumetric assessment is 96% - 97% while factor of error is 0.3 to 0.4% which is negligible, so we have enormous sort of results.

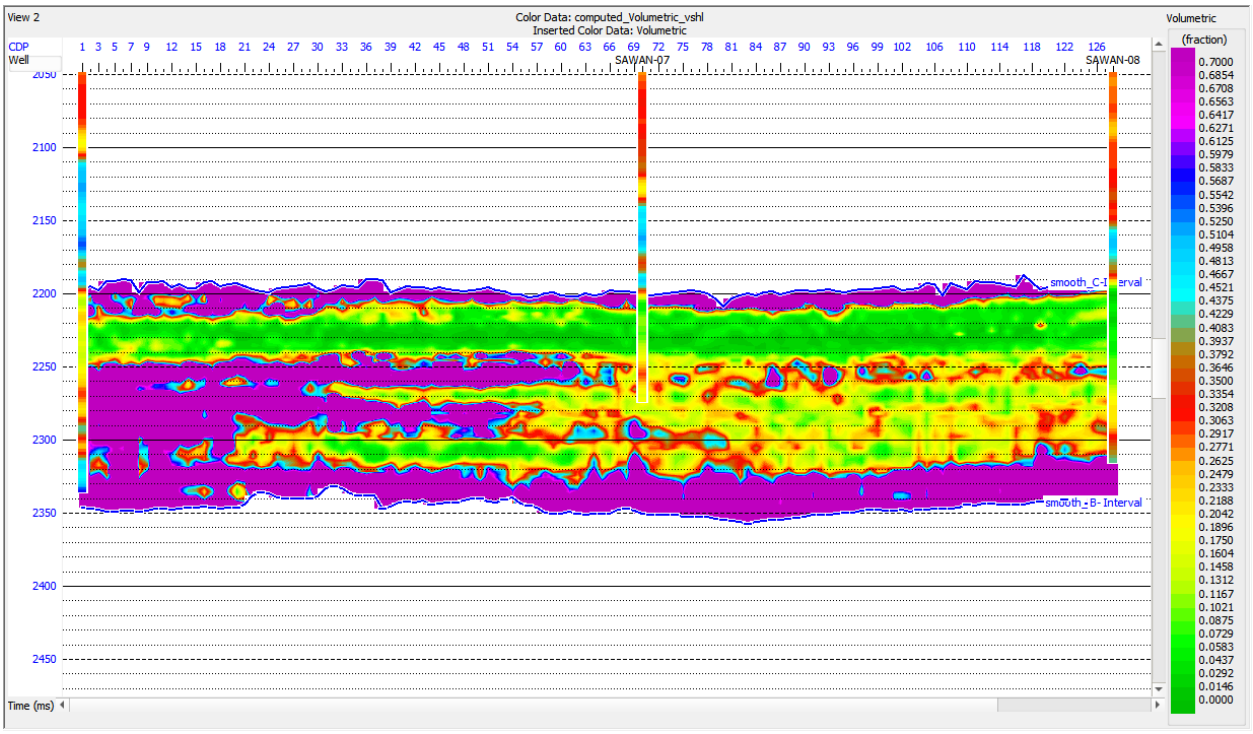

Figure 7.3 depicts that values ranging from 0.62 % to 0.68% which is holds very good results of C sand in Sawan-07.

7.3.1 Porosity prediction using PNN (Machine learning)

Estimation of porosity occurs from the inverted impedance and comparison occurred between actual porosity and modeled (predicted).

Porosity is predicted by probabilistic Neural Network. Correlation plot results of PNN for here is as follows in Figure 5.16. Actual porosity is showing good results in Modeled porosity and correlation is about 97%.

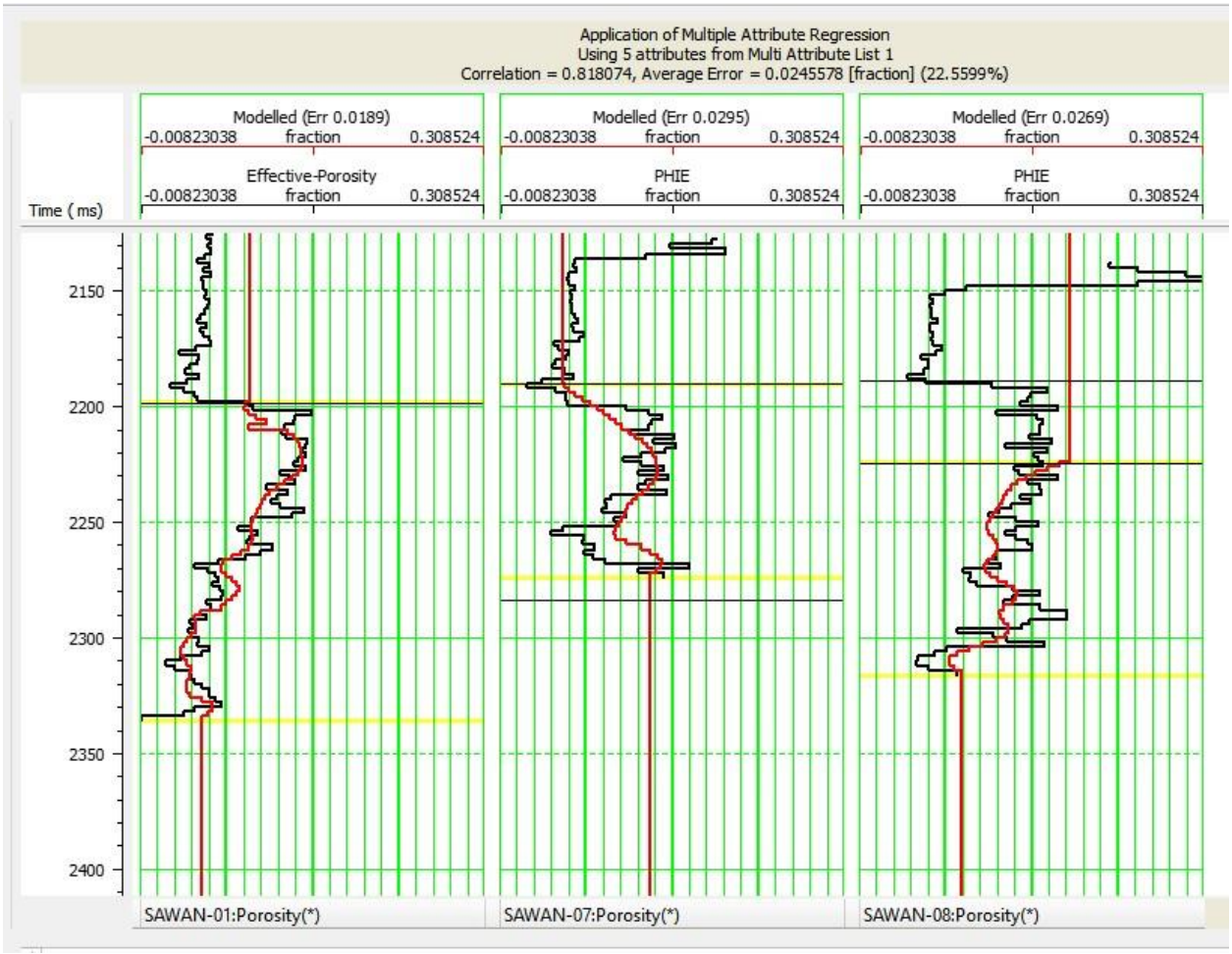

Figure 7.4 Training result of PNN modeled porosity(red) and actual porosity (black).

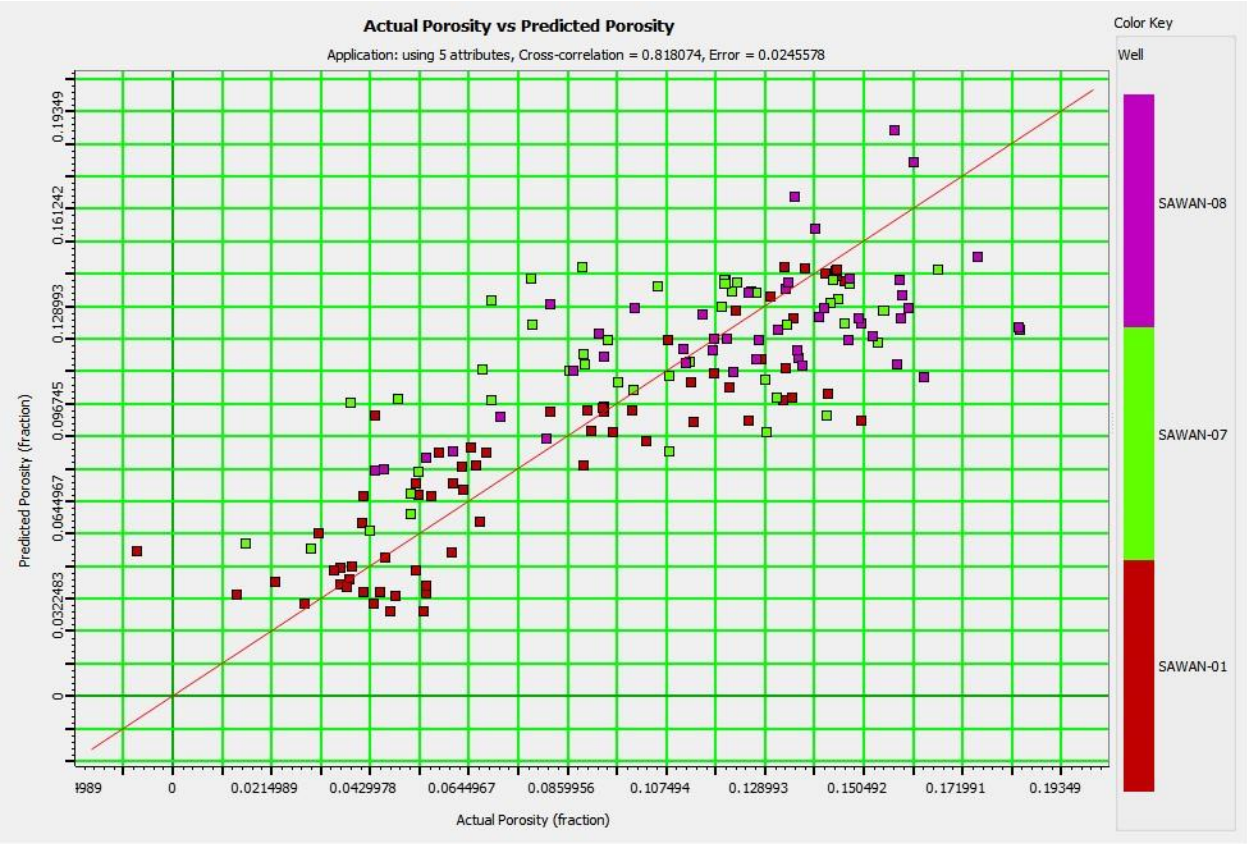

Figure 7.5 Cross plot of actual porosity and predicted porosity (modeled).

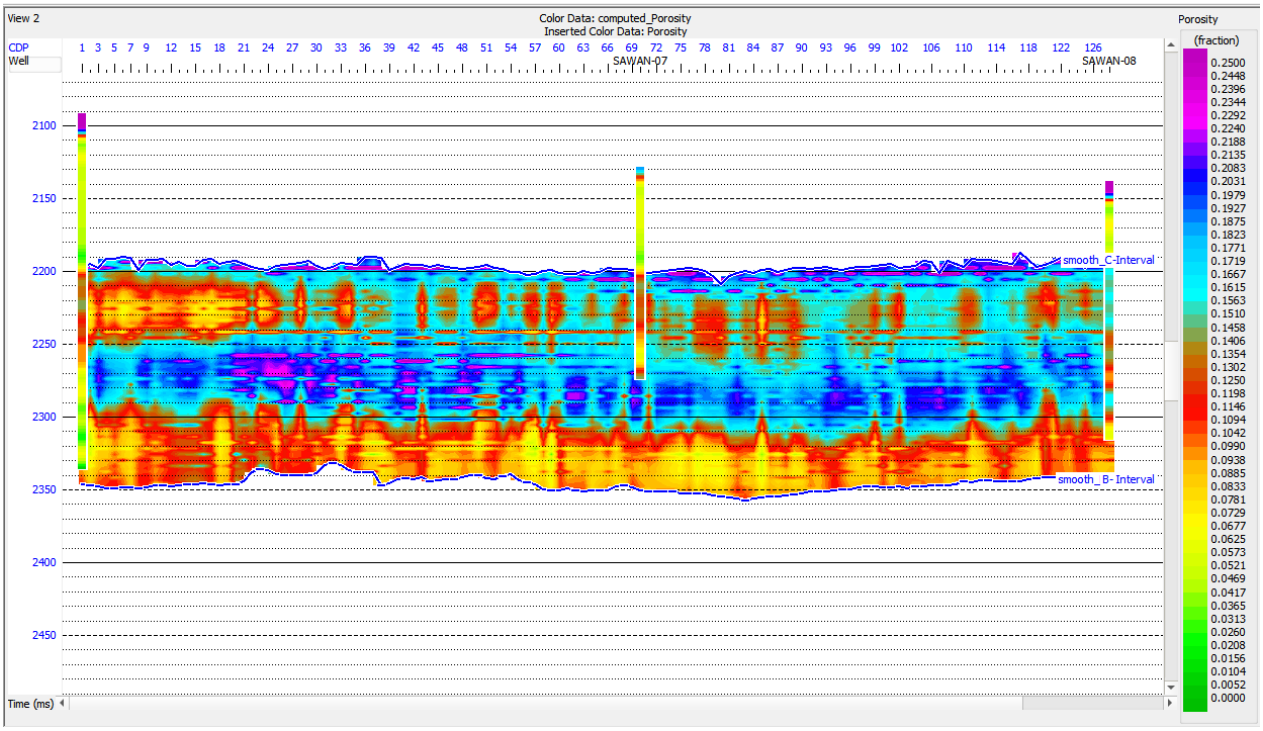

Figure 7.6 depicits that values ranging from 0.203 % to 0.215% porosity which is holding very good results of in C interval in Sawan-07.

7.3.2 Sw prediction using PNN (Machine learning)

Saturation of water is important parameter to depict Hydrocarbon potential of reservoir.As (1-SH = SW). So training error is 12% only which is negligible.

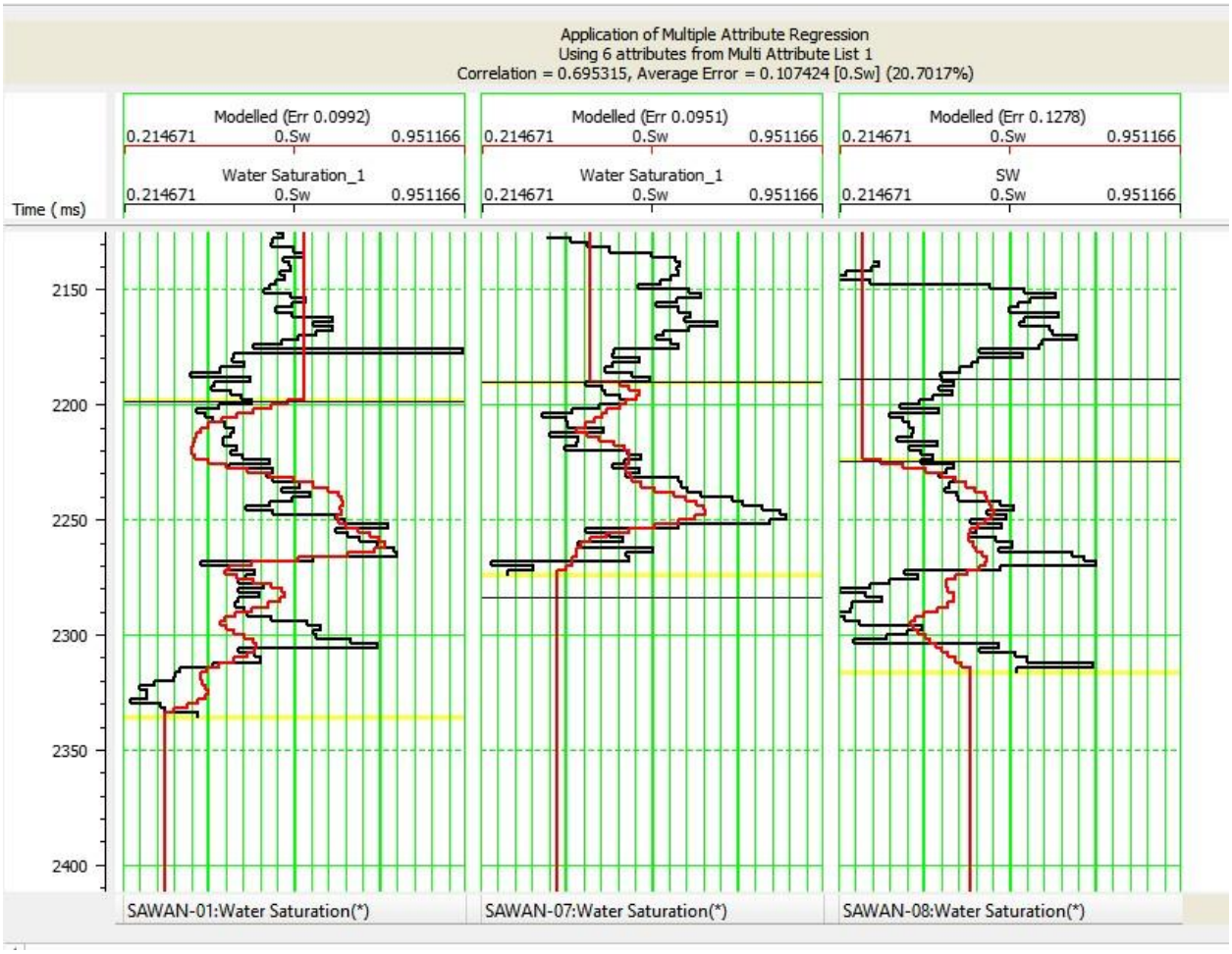

Figure 7.7 Training result of PNN modeled Saturation of Water, actual Saturation of Water.

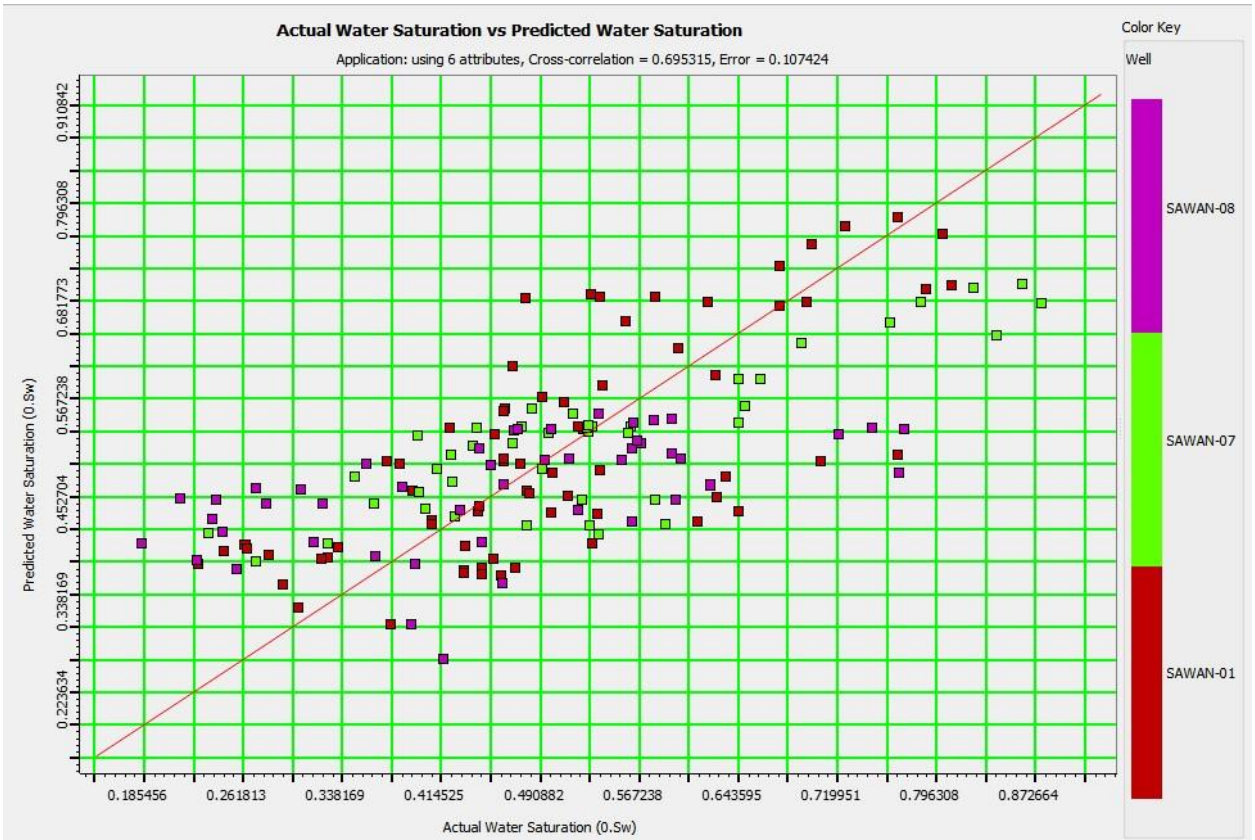

Figure 7.8 Cross plot of Actual Water Saturation with Predicted Water Saturation (modeled).

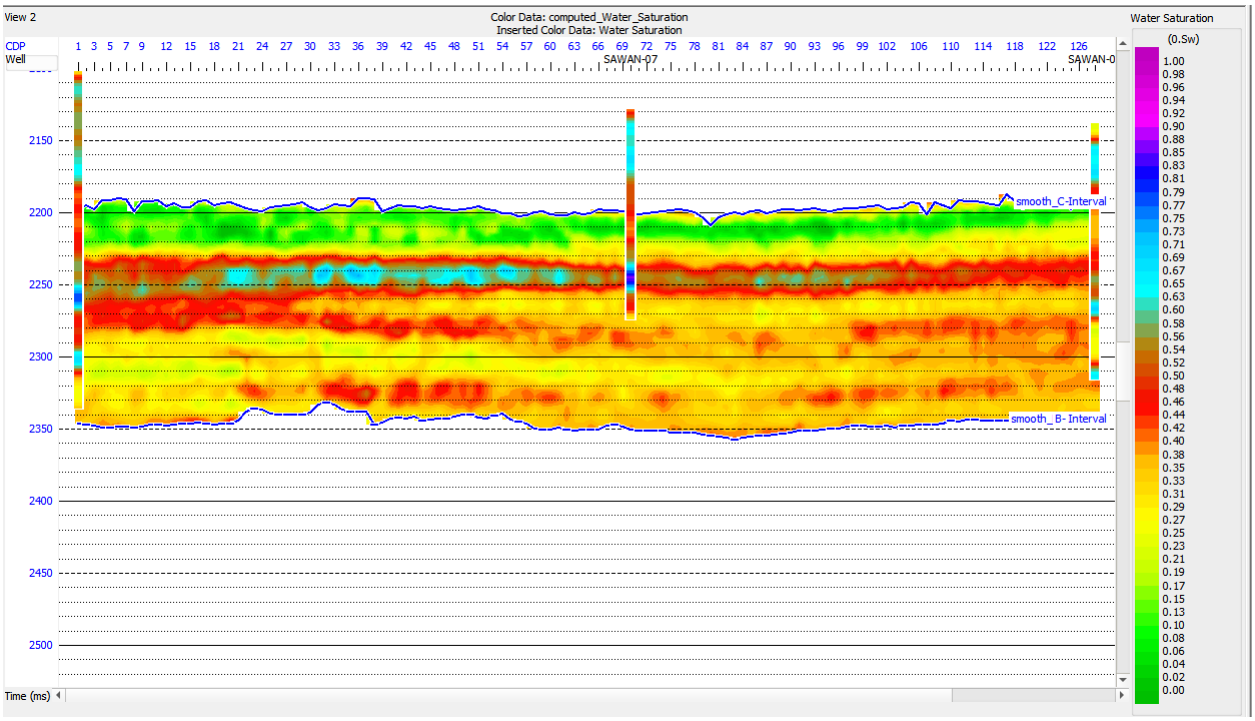

Figure 7.9 depicits that values ranging from 0.31% to 0.42% of predicted water Saturation which is holding very goodresults of C sand interval in Sawan-07.

CONCLUSIONS

1. 3D seismic interpretation has revealed that the study area is located in an extensional tectonic setting, characterized by the presence of two clearly defined normal faults on the seismic section. Additionally, when examining the time and depth contour maps, it becomes evident that the C interval exhibits a more pronounced behavior in terms of hydrocarbon presence compared to the B interval.
2. The petrophysical analysis of both Sawan 01 and Sawan 07 wells has identified distinct zones within the Lower Goru B and C Sands levels in both wells. In the C interval, hydrocarbon saturation (Sh) falls within the range of 71% to 86%, while in the B interval, Sh ranges from 30% to 50%. These findings suggest that the C interval possesses a greater potential for hydrocarbon accumulation.
3. Seismic inversion analyzed impedance changes in C and B intervals of the Lower Goru Formation. It identified a significant impedance drop at Sawan 01 and Sawan 07 along the C sand channel, suggesting possible hydrocarbon accumulation. In contrast, the B sand channel showed lower impedance only at Sawan 01, indicating higher hydrocarbon potential in the C interval.
4. Machine learning analysis, categorizing them into three distinct lithological packages: sand, shale, and tight sand.
5. Machine learning was applied in sequential steps. In the first step, the identified layer boundaries were utilized to compute the volume of shale from the gamma ray log, and a block averaging technique was applied within these boundaries.

REFERENCES

Abbasi, S.A., Kalwar, Z. and Solangi, S.H., 2016. Study of Structural Styles and Hydrocarbon Potential of Rajan Pur Area, Middle Indus Basin, Pakistan. Bu J ES, 1(1), pp.36-41.

Badley, M.E., 1985. Practical seismic interpretation.Blanford, W.T., 1883. Geological notes on the hills in the neighborhood of the Sindand Punjab Frontier between Quetta and Dera Ghazi Khan. Memoirs of the geological survey of India, 20, pp.105-240.

Bannert, D. and Raza, H.A., 1992. The segmentation of the indo-Pakistan Plate. Pakistan Journal of Hydrocarbon Research, 4(2), pp.5-18.

Colombo Plan Co-operative Project. Government of Canada for the Government of Pakistan.

Dobrin, M.B. and Savit, C.H., 1988. Introduction to Geophysical Prospecting.

Farah, A. and Lillie, R.J., 1989. Subsurface densities and lithospheric flexure of the Himalayan foreland in Pakistan. Tectonics of the Western Himalayas, 232, p.217.

Humayon, M., Lillie, R.J. and Lawrence, R.D., 1991. Structural interpretation of the eastern Sulaiman foldbelt and foredeep, Pakistan. Tectonics, 10(2), pp.299-324.

Hunting Survey Corporation, 1961. Reconnaissance Geology of Part of West Pakistan

Iqbal, M and Helmcke, D., 2004, Pakistan journal of Hydrocarbon Research, Vol 14, pg41-47, Geological interpretation of Earth quakes data of Zinda Pir Anticlinorium, Sulaiman Fold Belt,Pakistan).

Iqbal, M.W.A. and Shah, S.I., 1980. A guide to the stratigraphy of Pakistan (Vol.53).Geological Survey of Pakistan.

Jadoon, I.A., Lawrence, R.D. and Lillie, R.J., 1994. Seismic data, geometry, evolution, and shortening in the active Sulaiman fold-and-thrust belt of Pakistan, southwest of the Himalayas. AAPG bulletin, 78(5), pp.758-774.

Kadri, I.B., 1995. Petroleum geology of Pakistan. Pakistan Petroleum Limited.

Kazmi and Jan, 1997. Geology and tectonics of Pakistan. Graphic publishers. Kazmi, Snee, L.W. and Anwar, J., 1989. Emeralds of Pakistan: geology, gemology, and genesis. Van Nostrand Reinhold Company.

Kazmi, A.H. and Abbasi, I.A., 2008. Stratigraphy & historical geology of Pakistan (p. 524). Peshawar, Pakistan: Department & National Centre of Excellence in Geology.

Kemal, A., 1992. Geology and new trends for petroleum exploration in Pakistan. In Proc. Internat. Petroleun seminar on new directions and strategies for accelerating petroleum exploration and production in Pakistan (pp. 16-57).

Krois, P., Mahmood, T. and Milan, G., 1998, November. Miano field, Pakistan, A case history of model driven exploration. In Proceedings Pakistan Petroleum Convention (Vol.98, pp. 112-131).

Raza, H.A., Ahmed, R., Alam, S. and Ali, S.M., 1989. Petroleum zones of Pakistan. Pakistan Journal of Hydrocarbon Research, 1(2), pp.1-20.

Sarwar, G., 2004. Earthquakes and the neo-tectonic framework of the Kutch- Hyderabad Karachi triple junction area, Indo-Pakistan. Pakistan Journal of Hydrocarbon Research, 14, pp.35-40.

Serra, J., 1984. Descriptors of flatness and roughness. Journal of Microscopy, 134(3), pp.227-243.

Shami, B.A. and Baig, M.S., 2002. Geomodeling for the enhancement of hydrocarbon potential of Joya Mair field, Potwar, Pakistan. Pakistan Association of Petroleum Geoscientists-Society of Petroleum Engineers. In annual technical conference, Islamabad (pp. 124-145).

Sheriff, R.E. and Geldart, L.P., 1995. Exploration seismology. Cambridgeuniversity press.

Telford, W.M., Telford, W.M., Geldart, L.P., Sheriff, R.E. and Sheriff, R.E., 1990. Applied geophysics (Vol. 1). Cambridge University Press.

Wyllie, M.R.J., Gregory, A.R. and Gardner, G.H.F., 1958. An experimental investigation of factors affecting elastic wave velocities in porous media. Geophysics, 23(3), pp.459493